Impacts of Aviation Emissions on Air Quality Near Hanscom Field, Bedford, Massachusetts

Results of a Two-Season Monitoring Campaign

Prepared for

Hanscom Field Advisory Committee

and

Massport Community Advisory Committee

by

Environmental Monitoring Partners, LLC,
Lexington, MA

October 2025

Executive Summary

Introduction

Airports are a significant source of air pollution that can adversely impact air quality in downwind communities. The most commonly identified pollutants in aviation emissions include nitrogen dioxide, black carbon (or soot), ultrafine particles (UFP), and particulate lead. While much of the work to characterize emissions impacts has been performed near large, commercial airports, relatively few studies have been conducted at smaller general aviation airports. However, because residential areas are often located very close to general aviation airports where pollution levels are highest, it is important to characterize pollution dispersion patterns for the purpose of minimizing exposures.

To date, little work has been done to measure the impacts of aviation emissions from Hanscom Field (Bedford, Massachusetts) on the surrounding communities. We were tasked by the Hanscom Field Advisory Council (HFAC), the Massport Community Advisory Council (MCAC), and the Towns of Bedford, Lexington, Lincoln, and Concord to design and conduct a study to better understand the impacts of aviation emissions on the spatial and temporal distribution of air pollution in near-airport areas of each town.

Our objectives were to (1) measure UFP concentrations at stationary sites in each of the four towns during both cold and warm months, (2) map the spatial spread of air quality impacts measured using a mobile monitoring lab, and (3) collect and analyze particulate matter samples collected around the airfield for lead content. In addition, we also measured oxides of nitrogen and black carbon as part of the mobile monitoring effort.

Methods

UFP was monitored at eight sites around the airport including two sites in Lexington, two sites in Concord, three sites in Bedford, and one in Lincoln. The sites were located in residential areas as close as possible to flight paths and runways and as far as possible from busy roadways. Two to four sites on opposite sides of the airfield were operated concurrently to measure upwind and downwind differences in pollutant concentrations. Cold weather monitoring was conducted between February and April of 2024; warm weather monitoring was conducted between July and October of 2024. Lead and other elements were measured in samples collected at four sites including one in Lincoln, one in Concord, and two in Bedford.

Mobile monitoring was performed in all four towns using an electric vehicle equipped with rapid response instruments for measuring UFP, nitrogen dioxide, and black carbon and a GPS receiver to track location. Flight activity for the study period was obtained from FlightAware; meteorological data was obtained from the Integrated Surface Database and processed with US EPA's AERMET software.

Results

In total we monitored UFP at the stationary sites on 27-112 days per site, we performed mobile monitoring for 14 hours over four different days, and we collected 26 7-14-day samples for lead analysis. At the stationary sites we observed that hourly averaged UFP concentrations were as much as two-fold higher at downwind sites compared to upwind sites. Further, we found that the highest UFP concentrations occurred when the airfield was busy with flight activity. Overall, based on regional wind patterns we found that pollution levels were generally higher in Bedford and Lexington, which were downwind for much of the study period, compared to Lincoln and Concord, which were upwind. The Lexington sites were also impacted by local traffic and by emissions from Interstate-95, 1 mile to the west. The mobile monitoring results indicate that this impact was pervasive across hundreds of hectares in the downwind communities. Particulate lead concentrations were similar at all four sites and were not elevated relative to lead concentrations measured at a MassDEP air quality monitoring station in Boston; however, lead-to-bromine ratios were different at the Hanscom sites compared to the Boston site, suggesting different sources of lead at the two locations.

Implications

The UFP data indicate that Hanscom Field is having a deleterious impact on local air quality. In comparing our results to the World Health Organization guidelines, we found that UFP concentrations at Hanscom often exceeded the guidelines and did so more often when sites were downwind of the airport. The highest frequency of exceedances were at sites that were closest to the airfield. While our study was not designed to measure health impacts of Hanscom emissions on nearby communities, our results help to quantify current impacts, thereby providing a useful baseline dataset against which future proposed plans for changes to the airport and/or its operations can be evaluated. For example, we conclude (with a high

degree of confidence) that the proposed expansion of aviation activities at Hanscom[1] will lead to more frequent, prolonged, and severe exceedances of WHO air quality guidelines.

Possible follow-on actions

Based on our findings, we offer several possible follow-on actions for consideration.

1. Perform additional air quality monitoring at Hanscom Field, particularly at sites close to the ends of the runways where high UFP concentrations were observed (e.g., B1 and C2). While many kinds of monitoring campaigns could be considered, one option is to setup one or more long-term monitoring stations (much like MassDEP air quality monitoring stations) for measuring UFP and possibly other markers of aviation emissions (e.g., lead, nitrogen dioxide, benzene and other volatile organic compounds). Long-term monitoring would allow towns to keep better track of air quality in their communities and to use the data to inform decisions regarding proposed changes to aviation activities at Hanscom.

2. Perform indoor air quality monitoring for UFP in buildings near sites B1 and C2, where high UFP concentrations were measured in ambient air. Testing a variety of buildings – both public and private – of different ages, materials, architecture, and ventilation technologies could help to identify buildings (and building features) that are most and least susceptible to pollutant infiltration.

3. Develop a Logan-style Sound Insulation Program (https://www.massport.com/environment/noise-abatement/logan-airport/sound-insulation-program) as a way to reduce infiltration of airport-related air pollution (and noise) in homes near the airfield.

4. Develop outreach materials to better inform town government and residents of the impacts of airport-related emissions and potential health in their communities. Much of the information presented in this report requires an understanding of meteorology, aviation emissions, and pollutant transport in the environment. It is likely that some of the material in the report is not sufficiently explained to allow town officials and residents to completely grasp its significance. Therefore, investment in outreach materials that clearly explain the findings to a general audience

[1]EEA No. 16654 - L.G. Hanscom Field North Airfield Development, Bedford. https://eeaonline.eea.state.ma.us/EEA/MEPA-eMonitor/project/87734f7f-980d-4fd3-bdc8-2f3455089d61

(and place it in a larger context of planning for expansion of aviation activities at the airport) would lead to a more informed citizenry. Town-specific messaging may be important since aviation impacts are different in each of the towns.

5. Consider adopting land-use policies that help to reduce exposures to aviation-related air pollution near Hanscom, particularly for vulnerable populations. For example, promoting land-use buffers around the airfield and supporting roadway/traffic infrastructure, like what is currently being done with new schools near highways in California[2].

[2] California SB 352 (Escutia) of 2003, Source of Pollution at School Sites.

Acknowledgements

We are grateful to Manny Cabral, Kyle Walsh, Bradford Laing and the Diamond School in Lexington, Ron Scaltreto and John Glenn Middle School in Bedford, Kiah Walker and Jonathan Holdsworth at the National Park Service and Minuteman National Historic Park, and the generous homeowners for hosting our monitoring equipment. We are also grateful to Christopher Eliot and Aaron Toffler for logistical support. Sean Mueller conducted the metals analysis and assisted with data analysis and reporting; Arianna Cozza and Isabelle Berman assisted with data collection; Arianna Cozza and Camille Gimilaro assisted with data processing and generating data visualization products. Funding for this work was provided by the Towns of Bedford, Concord, Lexington, and Lincoln and the MassPort Community Advisory Committee.

Table of Contents

Executive summary 1
Acknowledgements 5
List of Tables 6
List of Figures 6
1.0 Ultrafine particles 9
1.1 Introduction 9
1.1.1 Objectives 10
1.1.2 Background 10
1.1.2.1 Summary of previous air quality studies at other airports 10
1.1.2.2 Ultrafine particles and health effects 12
1.1.2.3 WHO ultrafine particle guidelines 12
1.2 Methods 14
1.2.1 Hanscom Field 14
1.2.2 Air pollution monitoring and data analysis 14
1.2.3 Quality assurance 18
1.3 Results and Discussion 19
1.3.1 Overall Trends 19
1.3.2 Trends with respect to wind direction 19
1.3.3 Impact from a single aircraft operation event 21
1.3.4 Impacts on baseline air quality across neighborhoods 25
1.3.5 Seasonal differences 25
1.3.6 Exceedances of WHO guideline thresholds 30
1.4 Summary and Conclusions 34
2.0 Lead (Pb) 35
2.1 Introduction 35
2.1.1 Objectives 35
2.2 Methods 36
2.2.1 Quality assurance 39
2.3 Results and Discussion 39
2.3.1 Time-integrated PM2.5 mass measurements 39
2.3.2 Lead (Pb) concentrations and enrichment 41
2.3.3 Other aircraft-related metals: Br and As 41
2.4 Summary and Conclusions 45
3.0 References 46

List of Tables

Table 1.1 Monitoring locations, dates, definition of impact sectors, total hours of data collection. 17
Table 1.2 Summary statistics for hourly PNC at the stationary sites. 20
Table 1.3 Summary statistics for hourly PNC by site and wind conditions. 20
Table 1.4 Summary statistics for PNC for sites where measurements were made in two seasons. 30
Table 1.5 PNC exceedances of WHO UFP guidelines by site and wind conditions. 33
Table 2.1 Particulate matter sampling dates and numbers of samples collected. 37
Table 2.2 Mean particle mass concentrations. 40
Table 2.3 Concentrations of Pb, Br, As, and S (ng/m^3) in time-integrated PM samples. 42

List of Figures

Figure 1.1 Diurnal flight activity patterns at Hanscom Field. 15
Figure 1.2 Map showing locations of monitoring sites around Hanscom Field. 16
Figure 1.3 Windrose for Hanscom Field. 18
Figure 1.4 Hourly average PNC 'rose' for each site. 22
Figure 1.5 Box plots of PNC measurements collected simultaneously at paired sites. 23
Figure 1.6 Particle number concentration trends at three Bedford sites. 24
Figure 1.7 Particle number concentration trends at two Concord sites. 26
Figure 1.8 Spatial distribution of PNC based on 1-second measurements made on four days of mobile monitoring in 2023 and 2024. 27
Figure 1.9 Spatial distribution of NO_2 based on 10-second measurements made on two days of mobile monitoring in 2024. 28
Figure 1.10 Spatial distribution of black carbon based on 1-minute measurements made on two days of mobile monitoring in 2024. 29
Figure 1.11 PNC polar plots comparing cold weather and warm weather monitoring for three sites near Hanscom Field. 31
Figure 1.12 Bar charts showing mean 1-minute particle number concentrations for cold and warm months at two sites in Bedford and one in Lincoln. 32
Figure 2.1 Proportions of detections by element and monitoring site. 38
Figure 2.2 PM mass concentration by sample date and site. 40
Figure 2.3 Percentage of Pb, Br, As, and S content by particle size. 43
Figure 2.4 Concentrations of airborne Pb versus other elements. 44

List of Appendices

Table A.1. Sample size (hours) by season and monitoring site. 49

Figure A.1 Bar charts showing mean 1-minute PNC for various subsets of data. 50
Figure A.2 Hourly average PNC polar plot for each site in Bedford. 51
Figure A.3 Hourly average PNC polar plot for each site in Concord and Lincoln. 52
Figure A.4 Hourly average PNC polar plot for both sites in Lexington. 53
Figure A.5 Spatial distribution of ultrafine particles based on 1-second PNC measurements made on two days of mobile monitoring in July 2024. 54

Note to reader. *This report is organized into two main sections. The first section addresses ultrafine particles and the second section addresses lead. The reason for this division is that the methods used to measure and analyze the two pollutants are quite different, and it is hoped that by separating them in the narrative, it will make it easier for the reader to understand our methods and what the results mean.*

1.0 Ultrafine Particles

1.1 Introduction

It is widely reported that aviation emissions are a significant source of air pollution and that communities downwind of airports often experience adverse air quality impacts. While much of the work to characterize emissions impacts has been performed at relatively large, commercial airports (e.g., Los Angeles International Airport, Boston Logan International Airport, Schiphol Airport (the Netherlands), London Heathrow, Sea-Tac Airport in Seattle, Berlin-Tegel Airport (Germany), and TF Green Airport (Warwick, RI, USA) (Hudda et al. 2014; Hudda et al. 2016; Keuken et al. 2015; Stacey et al. 2020; Austin et al. 2021; Fritz et al. 2022; Hsu et al. 2012), to date few studies have been conducted at smaller general aviation airports (GAA). Nonetheless, despite the lower numbers of flights and smaller sizes of planes at GA airports compared to commercial airports, pollution exposures at GA airports can be significantly elevated because residential areas are often located very close to GAA airfields (e.g., <1,000 ft).

Exhaust from airplane engines contains complex mixtures of pollutants including gases (such as nitrogen dioxide, sulfur dioxide, and volatile organic compounds) and particulate pollutants (such as black carbon (soot) and ultrafine particles (i.e., particles <100 nanometers in diameter)) (Maisol and Harrison, 2014). In addition, propeller planes use leaded fuel; thus, emissions from propeller planes contain lead, typically in particle form (Griffith, 2020). While studies have shown that exposure to aviation emissions are associated with adverse health effects such as heart disease, cancer, cerebral and autonomic dysfunction, low birthweight, and asthma (Moreno-Ríos et al., 2022; Ohlwein et al., 2019; Schraufnagel, 2020), it is not known whether individual pollutants within mixtures or mixtures themselves are responsible for the observed health effects. Therefore, in characterizing pollutant exposures near airports, it is important that multiple pollutants be measured to better understand how pollutant co-variation may or may not impact health.

We were tasked with characterizing aviation emissions impacts in the four communities that abut the Laurence G. Hanscom Field (commonly referred to as Hanscom Field) in Bedford, Massachusetts. The communities include Lexington, Lincoln, Concord and Bedford. To our knowledge, this represents the first study of aviation emissions impacts on air quality in communities surrounding Hanscom Field.

Our goal was to design and conduct a study to measure the spatial and temporal distribution of chemical markers of aviation emissions in residential areas near the airport. In our study we used two common approaches: (1) we deployed monitoring equipment at stationary sites near flight paths and runways to collect measurements continuously (24 hours a day, seven days a week) for several weeks at each site, and (2) we used a mobile lab equipped with rapid-response monitoring equipment to measure the spatial patterns of pollutant impacts on selected neighborhoods in the four towns. In previous studies, we have found that the combination of stationary and mobile measurements can yield useful insights about pollution patterns that cannot be obtained if only one of the two methods is used without the other.

1.1.1 Objectives

We used ultrafine particles (UFP, particles with diameter <100 nm) as a marker of the spatial and temporal distribution of aviation emissions in communities near Hanscom Field. Ultrafine particles are indicative of fresh fossil fuel combustion emissions and are a useful marker of jet-engine exhaust near airports (Maisol and Harrison, 2014; Hudda et al., 2014). Our objectives were to

1. Monitor UFP at stationary sites in areas of the four towns that are close to Hanscom Airfield during both cold and warm months of the year.
2. Map the spatial distribution of air quality impacts measured using a mobile monitoring lab.
3. Analyze and interpret the data and report findings to stakeholders.

1.1.2 Background

1.1.2.1 Summary of previous air quality studies at other airports

It is well established that elevated noise exposures in near-airport communities can lead to adverse health impacts. For example, exposure to airport noise is associated with an increased risk of hypertension in a dose-dependent manner — meaning the more noise people are exposed to high levels of airport noise, the higher the risk of developing hypertension among the population (Jarup et al., 2008; Rosenlund et al., 2001; Babish et al., 2009). Research has also shown that people living in communities around airports are more likely to be taking prescription anti-hypertensive medication and have higher rates of cardiovascular disease, cardiovascular-related hospitalizations, and cardiovascular mortality (Franssen et al., 2004; Dimakopoulou et al., 2017; Correia et al., 2013; Huss et al., 2010). There is also evidence for adverse birth outcomes, increased rates of hospitalization due to respiratory diseases, and increased rates of learning deficits in children who live near airports (Matsui et al., 2003; Lin et al., 2008; Eagan et al., 2017).

In contrast to noise pollution, the adverse effects of airport-related emissions on ground-level air quality have not been well characterized. Aviation-related emissions are a significant source of UFP. Starting in 2014, the impacts of aviation emissions on ground-level ambient ultrafine particle concentrations were found to extend over unexpectedly large areas near airports, particularly along flight paths (Stacey, 2019). Since then, many studies have demonstrated that aviation exhaust is a major source of UFP pollution in downwind communities. For example, elevated UFP concentrations were reported downwind as far as 4.5 miles of Logan Airport in Boston, 10 miles of Sea-Tac Airport in Seattle and 12 miles of Los Angeles International Airport (LAX) (Hudda et al., 2016; Austin et al., 2021; Hudda et al., 2014).

UFP concentrations around Los Angeles International Airport (LAX) were at least two times higher than typical background as far as 12 miles downwind and were five times higher within 5 miles of LAX (Hudda et al., 2014). The level of increase in UFP near LAX was found to be equivalent to emissions from 25% of all highways and freeways in Los Angeles County. Similarly, at locations 2.5 miles and 4.5 miles from Logan Airport in Boston (BOS), UFP concentrations were 100% and 33% higher, respectively, when winds were from the direction of the airport compared to other directions (Hudda et al., 2016). Further, UFP concentrations were positively correlated with flight activity and increased with increasing wind speed, suggesting that aircraft exhaust plumes were the likely source.

It has also been shown that airport-origin UFP can penetrate into residences and that impacts are particularly large for homes under flight paths. For example, in a study of 16 residences located in the greater Boston metropolitan area 2-6 miles from BOS, the median indoor concentrations of ultrafine particles were 70% higher when homes were downwind of the airport (Hudda et al., 2018). At a residence near BOS, under the flight trajectory of the most utilized runway, Hudda et al. (2020) reported that when the residence was downwind of the airport the concentrations of ultrafine particles, oxides of nitrogen (NO, NO_2 and NO_X), black carbon, and polycyclic aromatic hydrocarbons were 1.1- to 4.8-fold higher. In fact, NO_2 concentrations at the residence exceeded those measured at regulatory monitoring sites in the area including one adjacent to an interstate highway. Further, the impacts were highest during landings: the average UFP concentration was 7.5-fold higher from landings versus takeoffs on the closest runway. In addition, UFP concentrations inside the residence were only 30% lower than concentrations outdoors, indicating there was substantial infiltration of aviation-origin emissions and that residential building envelopes did not provide adequate protection from this air pollution. Infiltration resulted in indoor UFP concentrations that were comparable to ambient concentrations measured locally on roadways and on interstate highways.

Similarly, at LAX the highest UFP concentrations were detected at locations under landing jets and consisted mainly of UFP smaller than 40 nanometers (Hudda et al., 2016). The predominance of smaller sized particles in the impacted areas increased lung deposition fractions by 15-40% (Hudda et al., 2016). The uniquely small size of particles associated with airport-origin air pollution was also observed in Seattle under flight paths up to 10 miles downwind of Sea-Tac Airport (Austin et al., 2021).

1.1.2.2 Ultrafine particles and health effects

Exposure to UFP has been shown to adversely impact human health. Due to their small size, UFP can be inhaled deeply into the lungs causing inflammation, and it can enter the bloodstream and become widely distributed in many parts of the body. Particle size has been correlated with total and cardiovascular mortality, with studies suggesting that the smallest diameter particles may be disproportionately responsible for adverse health effects (HEI, 2013; Ohlwein et al., 2019).

For example, an increased risk of pre-term birth was reported for women who lived near LAX and were exposed during pregnancy to higher concentrations of UFP from aircraft (Wing et al., 2020). An increased risk of malignant brain cancer in residents was also found in people who lived near LAX and were exposed to higher levels of UFP from aircraft activity (Wu et al., 2021). In a study of short-term effects, exposure to LAX-related UFP was associated with increased levels of IL-6 (a blood marker of inflammation) in adult asthmatics following mild walking activity (Habre et al., 2018). Also, in a study that took place near Schiphol Airport (Amsterdam, The Netherlands), short-term exposure (five hours) to aviation-related ultrafine particles was also associated with decreased lung function in healthy young adults (Lammers et al., 2020). These studies add to the growing epidemiological evidence that aviation-related UFP exposures are harmful to human health.

1.1.2.3 WHO ultrafine particle guidelines

The World Health Organization (WHO) has recently weighed in on the question of regulating UFP in ambient air and establishing air quality limits for UFP:

> "*Since [….2005], the body of epidemiological evidence [on UFP] has grown, and two systematic reviews have assessed scientific research papers published from 1997 to 2017 (HEI, 2013; Ohlwein et al., 2019), documenting the rising number of studies being conducted. The studies demonstrated short-term effects of exposure to UFP, including mortality, emergency department visits, hospital admissions, respiratory symptoms, and effects on pulmonary/systemic inflammation, heart rate variability and blood pressure; and long-term effects on mortality (all-cause, cardiovascular, IHD and pulmonary) and several types of morbidity. However, various UFP*

size ranges and exposure metrics were used, preventing a thorough comparison of results across studies (US EPA, 2019a). Therefore, there was a consensus in the GDG [Guideline Development Group] that the body of epidemiological evidence was not yet sufficient to formulate an AQG [Air Quality Guideline] level.

At the same time, however, there is a large body of evidence from exposure science that is sufficient to formulate good practice advice. The most significant process generating UFP is combustion and, therefore, the main sources of the UFP include vehicles and other forms of transportation (aviation and shipping), industrial and power plants, and residential heating. All of these utilize fossil fuels and biofuels, as well as biomass. Since everyone is exposed to the emissions from these sources, exposure to UFP is of concern."[3]

The WHO has issued four 'good practice' statements on UFP to guide decision-makers and researchers towards reducing ambient UFP concentrations.

1. *Quantify ambient UFP in terms of particle number concentration (PNC) for a size range with a lower limit of ≤10 nm and no restriction on the upper limit.*
2. *Expand the common air quality monitoring strategy by integration of UFP monitoring into existing air quality monitoring. Include size-segregated real-time PNC measurements at selected air monitoring stations in addition to, and simultaneously with, other airborne pollutants and characteristics of PM.*
3. *Distinguish between low and high PNC to guide decisions on the priorities of UFP source emission control. Low PNC can be considered <1,000 particles/cm^3 (24-hour mean). High PNC can be considered >10,000 particles/cm^3 (24-hour mean) or 20,000 particles/cm^3 (1-hour mean).*
4. *Utilize emerging science and technology to advance approaches to the assessment of exposure to UFP for application in epidemiological studies and UFP management."*[4]

In this report we compare our results to these guidelines.

[3] WHO global air quality guidelines: Particulate matter (PM2.5 and PM10), ozone, nitrogen dioxide, sulfur dioxide and carbon monoxide [Internet]. Show details Geneva: World Health Organization; 2021. URL: https://www.ncbi.nlm.nih.gov/books/NBK574595/

[4] https://www.ncbi.nlm.nih.gov/books/NBK574595/box/ch4.box15/?report=objectonly

1.2 Methods

1.2.1 Hanscom Field

Hanscom Field (KBED), located 20 miles northwest of Boston, is the largest public use general aviation airport in New England. Hanscom Field has two runways: the primary runway, 11/29, is 1.3 miles long (2.14 km) and oriented northwest to southeast, and the secondary runway, 5/23, is 0.95 miles long (1.53 km) and oriented southwest to northeast. During our monitoring campaign, the airport averaged 271 operations per day, with most of the activity representing transient and local general aviation. Diurnal trends in flight activity at Hanscom Field during the study period are shown in Figure 1.1.

1.2.2 Air pollution monitoring and data analysis

Air pollution was monitored at eight stationary sites, which were selected to represent the Hanscom-abutting communities of Lexington (n=2 sites), Concord (n=2 sites), Bedford (n=3 sites), and Lincoln (n=1 sites) (see Figure 1.2). Of these, five were institutional sites (including two public schools) and three were residential sites. In our figures, we have purposefully not included the basemap and the spatial scale and we jittered the residential site locations by a small distance to protect the privacy of the residents. In addition to stationary-site monitoring, we also performed mobile monitoring in all four towns using an electric vehicle equipped with fast-response instruments. To identify seasonal differences in air pollution patterns at Hanscom, monitoring was performed in two campaigns: a cold-weather campaign (February 6 to April 28, 2024) and a warm weather campaign (July 12 to October 31, 2024).

Ambient PNC was monitored using water-based condensation particle counters (CPC; TSI Inc. Model 3783, lower size limit of 7 nm) housed inside temperature-controlled shelters. At one stationary site, we also used a butanol-based CPC (Model CPC 3775, lower size limit of 4 nm). PNC measurements were recorded every second. Data from the CPCs were processed to remove measurements that were automatically flagged as being erroneous. The most common errors (and reasons for removing data) were caused by nozzle pressure faults, pulse height faults, and instrument temperatures being out of range. We also removed all PNC readings <100 particles/cm^3. Processed data were aggregated to minutely and hourly resolution. Using the methods described in Hudda et al. (2016), we classified the data as being in the '*impact sector'* if the wind was such that it swept over the airport causing stationary sites or mobile monitoring routes to be directly downwind of the airport and *'non-impact sector'* otherwise. However, this approach requires non-calm winds for classification. During calm winds (i.e., <0.5 m/s or ~1 mph), we

expect the sites to be impacted more by sources in the immediate

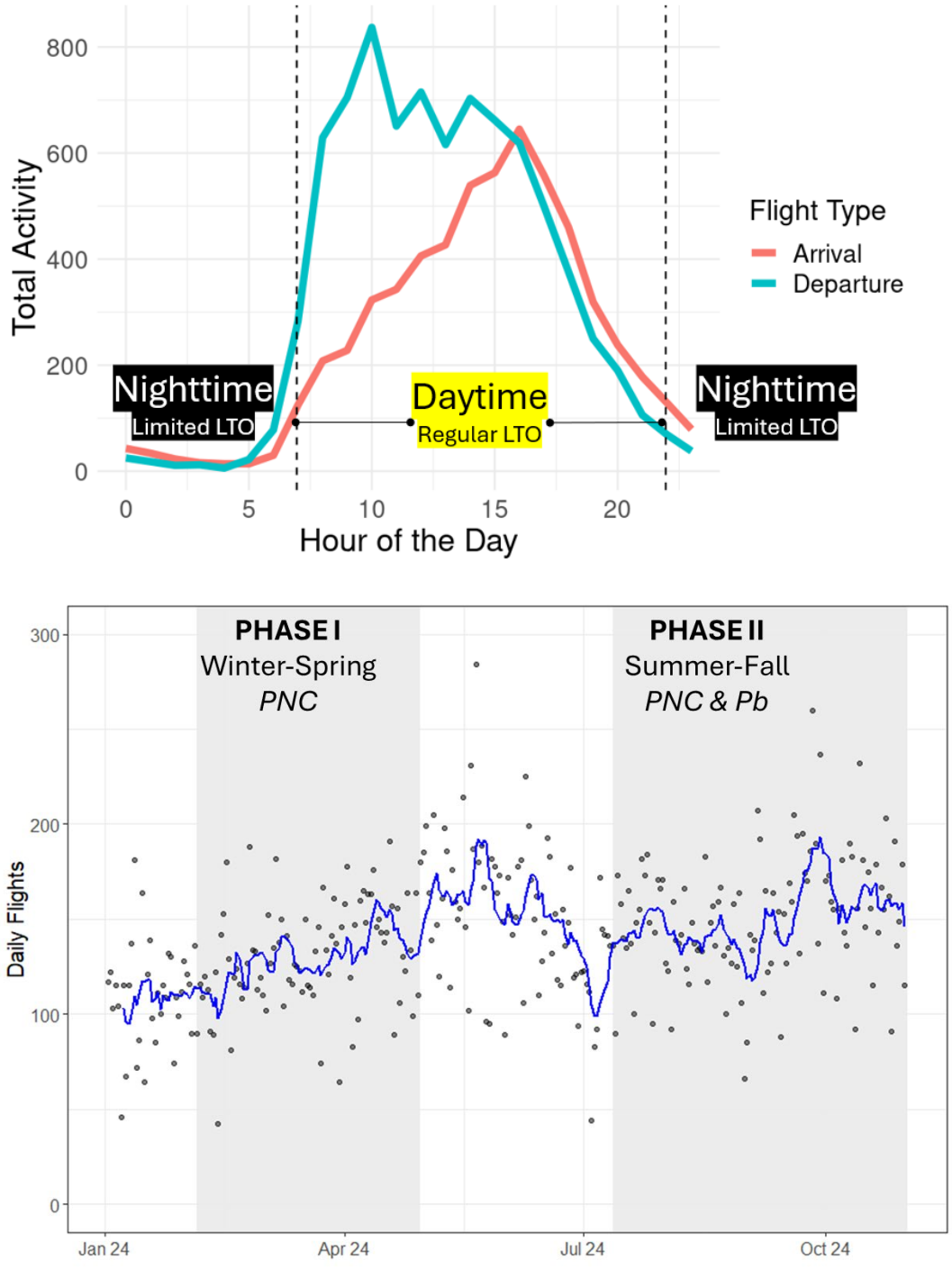

Figure 1.1 Fight activity at Hanscom Field. Upper panel shows total flight activity (all flights during the period 1/25/2024 to 10/31/2024) for each hour of the day. Lower panel shows daily total flight activity for each day throughout the study period; blue line represents loess smooth. LTO stands for landings and takeoffs. "Limited" means there are much fewer flights during these times compared to "Regular" hours of operation.

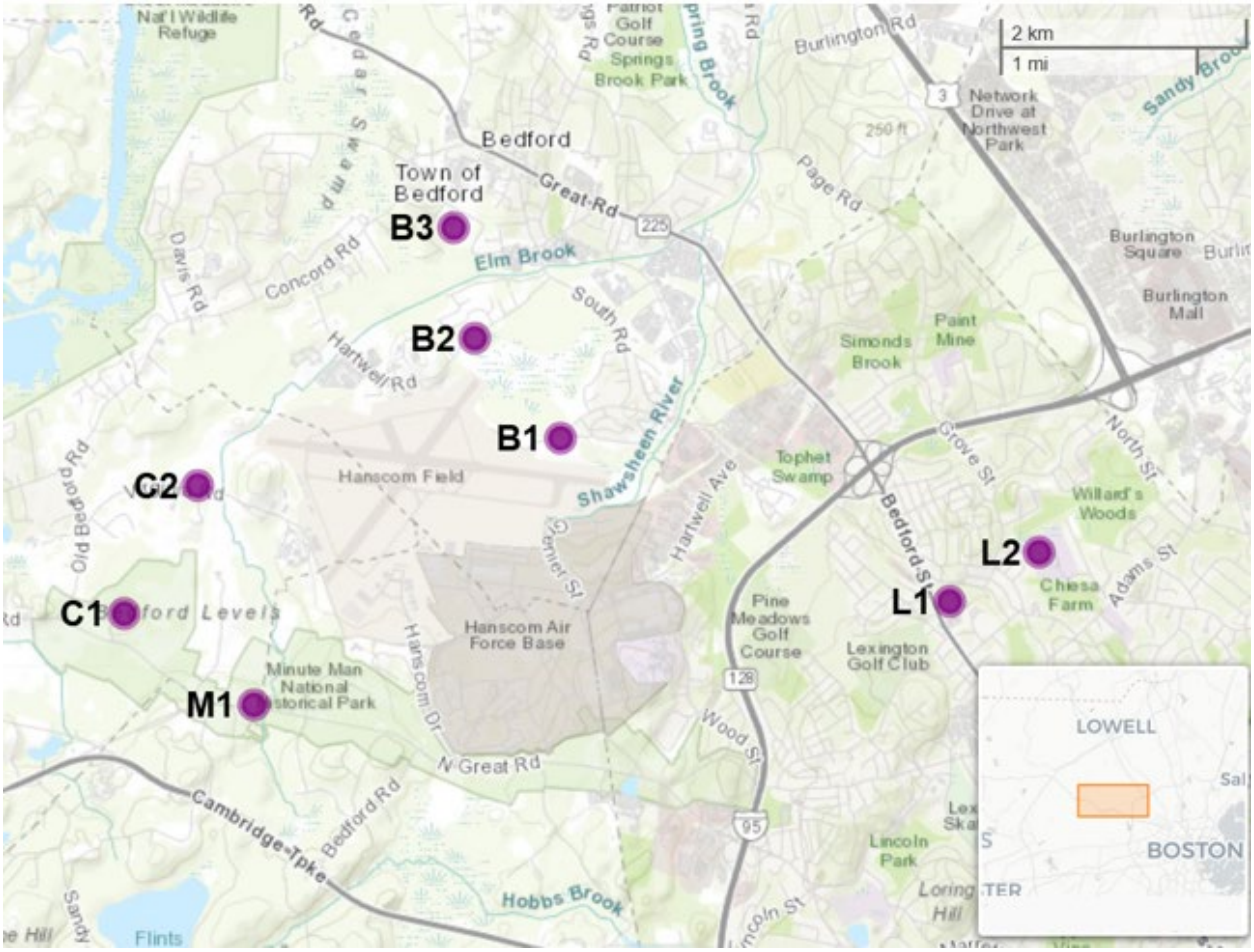

Figure 1.2 Map of the study area and locations of the stationary monitoring sites.

vicinity of the site, which might or might not be the airport depending on the location. Data collected during calm winds was differentiated and reported separately in tables and graphics where necessary (e.g., Figure 1.3 and Table 1.1). Further, at site B1, which is very close to the airport, we use the approach of categorizing data for a 180-degree-wide sector relative to the airport as the 'impact sector,' as demonstrated in our previous work at a general aviation airport (Hudda et al., 2022).

Mobile monitoring was performed using a battery electric vehicle that was equipped with six marine deep-cycle 12-VDC batteries and an inverter that provides 120 VAC to power the onboard instruments. The vehicle contained an air sampling manifold to which pollutant monitoring instruments were plumbed. Ambient air was conveyed from the inlet mounted in the right rear window and through the manifold by two identical fans on either end of the manifold. Separate lines for each instrument were connected to the manifold upstream of the inlet fan. A TSI Model 3783 condensation particle counter (CPC) was used to measure ultrafine particles, an aethalometer (Model AE33, Magee Scientific, Berkeley, CA) was used

Table 1.1 Monitoring location, dates, definition of impact sector and total hours of data collected under different wind conditions.

Sites	Town	Impact sector[1]	Cold weather monitoring dates (2024)	Warm weather monitoring dates (2024)	Distance[2]	Total hours of data[3]
Bedford Private Residence - B1	Bedford	135°-315°	3/3-4/16	8/21-10/31	900	IS:1277 NIS:880 Calm:213
Bedford Private Residence - B2	Bedford	138°-245°	3/8-4/26	9/10-9/24	1,800	IS:184 NIS:877 Calm:144
Glenn Middle School, Bedford - B3	Bedford	144°-222°	3/20-4/16	NM	4,800	IS:41 NIS:338 Calm:82
Concord Private Residence - C1	Concord	38°-75°	2/25-3/29	NM	5,400	IS:55 NIS:344 Calm:86
Thoreau Farm - C2	Concord	55°-90°	3/8-4/25	NM	2,100	IS:85 NIS:736 Calm:137
Minuteman National Park - Job Brooks House, M1	Lincoln	2°-58°	3/29-4/28	7/12-9/10	3,700	IS:114 NIS:1225 Calm:171
Hadley DPW Building, L1	Lexington	272°-292°	2/6-3/8	NM	9,700	IS:58 NIS:502 Calm:135
Diamond Middle School, L2	Lexington	268°-289°	2/6-3/8	NM	11,700	IS:48 NIS:440 Calm:123

[1]When winds are coming from these directions, site is in the airport impact sector (IS).
[2]Shortest distance (feet) from the monitoring site to the nearest edge of the nearest runway.
[3]NIS = non-impact sector.
NM = no monitoring was performed at this site during the warm weather monitoring period.

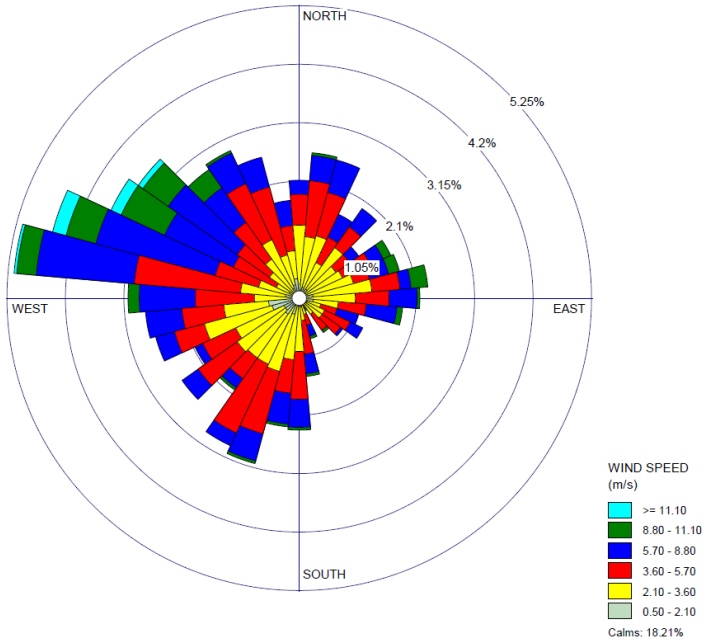

Figure 1.3 Windrose for Hanscom Field based on wind speed and direction measurements.

for measuring black carbon, a Cavity Attenuated Phase Shift (CAPS) nitrogen dioxide monitor (Aerodyne Research, Billerica, MA) was used for NO_2. PNC and NO_2 measurements were collected at 1-second resolution while black carbon (BC) measurements were collected every minute. Individual measurements were mapped to location by 1-second GPS readings (Model GPSMAP 64sx, Garmin Ltd., Olathe, KS). Data processing procedures for mobile measurements were followed as described by Hudda et al. (2020).

Hourly landing and takeoff (LTO) data for the study period were obtained from FlightAware (https://www.flightaware.com/), and meteorological data collected at Hanscom were obtained from the Integrated Surface Database (https://www.ncei.noaa.gov/products/land-based-station/integrated-surface-database).

1.2.3 Quality assurance

We performed regular instrument checks and preventive maintenance in the field. Briefly, each stationary site was visited weekly. During each visit the CPCs were maintained by refilling the distilled water reservoir, downloading the data from the previous week, adjusting the temperature inside the shelters as needed, changing wicks and cleaning nozzles as needed, and resetting CPC clocks. Prior to the start of the study, one of the CPCs was factory calibrate, and then a side-by-side test was performed to ensure that the other CPCs measured to within 10% of the calibrated CPC. Flow checks and zero checks were performed regularly for all instruments. During data processing, we applied instrument-specific

algorithms to remove erroneous measurements. Overall, we met our study goal for completeness: over 90% of measurements met our data quality objectives.

1.3 Results and Discussion

1.3.1 Overall trends

As shown in Table 1.1, we collected UFP measurements at eight sites during 82 days of the cold-weather study period (February 6 to April 28, 2024). During this time, UFP measurements were collected for 49 days in Bedford (n = 3 sites), 48 days in Concord (n = 2 sites), 31 days in Lexington (n = 2 sites), and 30 days in Lincoln (n = 1 site). During the warm-weather campaign (July 12 to October 31, 2024), UFP measurements were collected for 79 days in Bedford (n = 2 sites) and 49 days in Lincoln (n = 1 site). Together, this amounted to 293 total monitor-days[5] during the cold-weather campaign and 128 total monitor-days during the warm-weather campaign. Whereas during the cold-weather campaign we monitored at eight sites to better characterize the spatial distribution of emissions around the airport, during the warm-weather campaign we monitored at fewer sites (n = 3) based on the assumption that only temporal patterns would differ across the seasons while spatial patterns would generally be the same. In the sections that follow, we use these measurements to describe the impacts of aviation activities at Hanscom on air quality in the four towns. Emphasis is placed on describing the impacts of aviation activities on baseline air quality across the four towns, describing trends with respect to predominant wind directions, showing the impacts of individual aircraft operations on air quality, and comparing our findings to relevant air quality guidelines for UFP.

1.3.2 Trends with respect to wind direction

In general, the highest particle number concentrations (PNC) were observed at the sites that were closest to Hanscom Field (B1, B2, M1, C1 and C2) (Tables 1.2 and 1.3). Also, we observed higher PNC during calm or very light winds and during winds that oriented these sites downwind of the airport (i.e., during impact sector winds) compared to higher wind speeds and winds that oriented the sites upwind of the

[5] A 'monitor-day' is the sum of all monitors operating across all days of monitoring. Thus, for example, if 4 monitors are collecting measurements simultaneously over the course of ten days, then that period counts as 40 monitor-days.

Table 1.2. Summary statistics for hourly PNC at stationary sites.

Site	Mean (stdev)	Median (iqr)
B1	8600 (7700)	6200 (7300)
B2	5300 (4000)	4200 (4200)
B3	6400 (4600)	5300 (5100)
C1	6200 (4300)	5200 (4200)
C2	7500 (7200)	5100 (5600)
M1	5500 (3800)	4400 (3700)
L1	7800 (4500)	6900 (5800)
L2	5500 (3200)	4900 (3700)
B1 butanol[1]	9800 (8300)	7700 (8600)

Stdev = standard deviation
Iqr = interquartile range
[1]A butanol CPC (TSI model 3775; lower particle size = ~4 nm) was used at this site for four weeks.

Table 1.3. Summary statistics for hourly PNC by site and wind conditions.

Site	Impact sector		Non-Impact sector		Calm	
	Mean (stdev)	Median (iqr)	Mean (stdev)	Median (iqr)	Mean (stdev)	Median (iqr)
B1	9300 (8600)	6700 (8000)	6800 (5300)	5100 (5100)	11800 (8500)	9900 (9700)
B2	7800 (5800)	6300 (6500)	4600 (3300)	3700 (3600)	6400 (3500)	5800 (4100)
B3	9100 (6500)	7300 (5000)	5600 (4100)	4400 (4700)	8400 (4100)	6700 (4800)
C1	7300 (4000)	6400 (5800)	5700 (4500)	4800 (4000)	7200 (3300)	6800 (4200)
C2	15600 (11300)	12400 (14800)	6500 (6400)	4400 (4500)	7500 (4900)	6000 (3800)
M1	7200 (5200)	6000 (5400)	5200 (3600)	4200 (3600)	6000 (3500)	5000 (3000)
L1	6300 (4200)	5100 (4500)	7000 (3800)	6200 (4700)	11400 (5300)	10900 (6500)
L2	5100 (3400)	3700 (4200)	5000 (2700)	4500 (2900)	7100 (3900)	6500 (4100)
B1 butanol[1]	9600 (8900)	6200 (9900)	8000 (5600)	6600 (6300)	16200 (11200)	12700 (10600)

Stdev = standard deviation; Iqr = interquartile range
[1]A butanol CPC (TSI model 3775; lower particle size = ~4 nm) was used at this site for four weeks.

airport (i.e., non-impact sector winds). Also, we observed higher concentrations during daytime hours when there was greater flight activity. Tables 1.2 and 1.3 and Figures 1.4 and A.1-A.4 summarize these broad trends across all the sites. Each colored dot in Figure 1.4 (and Figures A.2-A.4) represents the mean of one hour of PNC measurements plotted against the corresponding wind speed and wind direction for the hour. Calm-wind data is plotted at the center of the figure (i.e., at zero wind speed) even though calms are defined as <0.5 m/s winds. In contrast to the near-airfield sites, we observed some of the lowest airport impact sector concentrations at the two Lexington sites (L1 and L2), which were the farthest of all the sites from the airfield (Tables 1.1 and 1.3). The high concentrations during calm winds at site L1, which was on the roof of the Lexington Department of Public Works building, suggest a local emissions source – for example, emissions from heavy duty vehicles moving in and out of the garages at the facility.

It is interesting to note the contrast between the Concord and Bedford sites located along runway 5/23 in Figure 1.5. At site C2 in Concord, which is upwind of the airport during westerly winds, we recorded some of the lowest concentrations during westerly winds. As westerly winds sweep across the airfield, they pick up airport emissions and disperse them to the east. Thus, the same westerly winds during which we observed relatively clean air at upwind sites in Concord are associated with some of the highest PNC measurements at sites in Bedford – particularly sites B1 and B2, which are downwind of the airport in westerly winds. The situation reverses during easterly winds: Bedford sites record lower concentrations during easterly winds and Concord sites their highest. A similar contrast is observed between Lincoln (M1) and Bedford (B2) sites located along the 11/29 primary runway during southwesterly and northeasterly winds (Figure 1.5).

Concentration differences between paired upwind and downwind sites can also inform us of the magnitude of the impact that Hanscom's operations has on pollutant concentrations. For example, cold weather monitoring indicates that median hourly PNC is 2,000-4,000 particles/cm^3 higher (i.e., ~70% higher) for the downwind sites compared to the upwind site for each pair.

1.3.3 Impact from a single aircraft operation event

The impacts from a single jet aircraft's operation on air quality were tracked and quantified in the vicinity of the airport. Discrete emissions plumes from individual aircraft operations (takeoffs, landings, idling, taxiing) can be measured near the airport fence line and manifest as sharp increases (or spikes) in concentration, which can be on the order of 100 ppm for CO_2 (or 25% increase over background) to ~100,000 particles/cm^3 for ultrafine particles (or ~10-fold increase over background). These spikes are

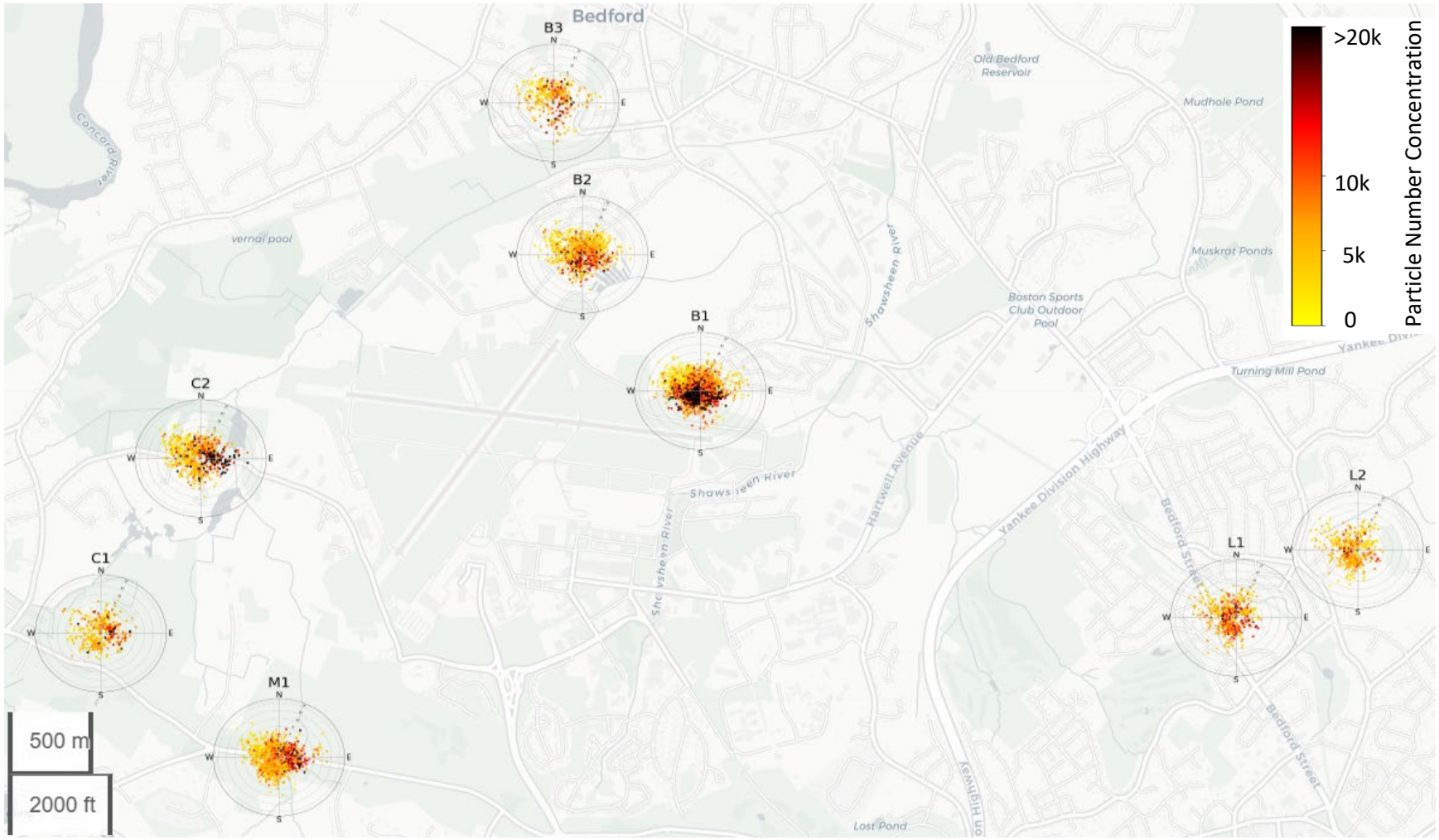

Figure 1.4 Hourly average PNC polar plot for each site. PNC is expressed in units of particles/cm^3 of air. The angular coordinate indicates the direction from which the wind is blowing, while the radial axis represents wind speed. Each point represents one hour of data; the points are colored according to the hourly average concentration. See Figures A.2-A.4 for a close-up view of the polar plots.

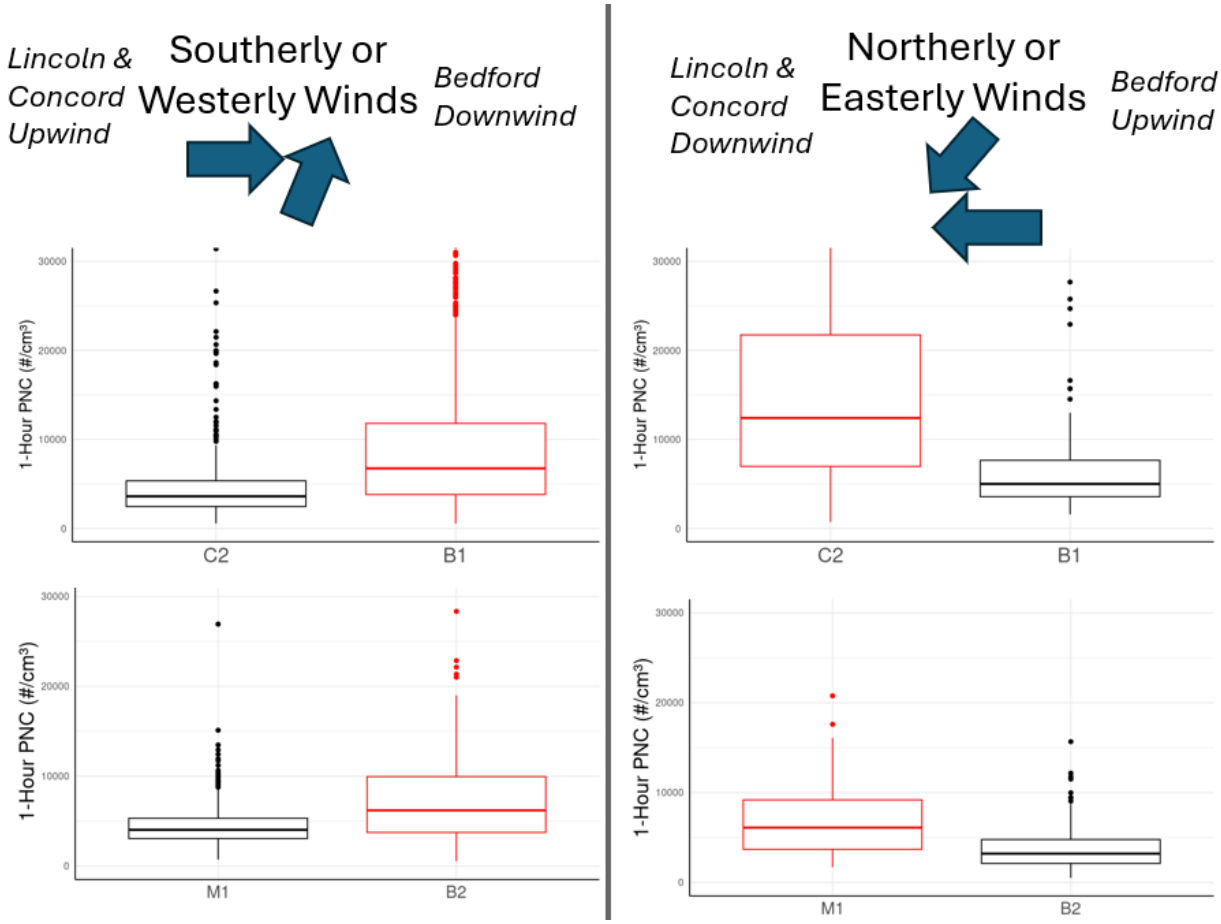

Figure 1.5 Box plots of PNC measurements collected simultaneously at paired sites under different wind conditions. Red boxes are from sites downwind of the airfield; black boxes are from sites upwind of the airfield.

followed by equally sharp decreases in concentration a few seconds or tens of seconds later. An example of such an event in Figure 1.6 shows that as the plume disperses, the spikes dissipate with displacement of the plume to another location by either its own momentum (due to the force imparted to plumes as they exit engines) or advection by wind. The magnitude of the spike depends on many factors including aircraft age and type, thrust level, fuel type, and importantly the distance of the measurement location to the aircraft. All of this results in large event-to-event variation in near-fence-line pollutant concentration measurements. This approach (i.e., making measurements at locations around the airport fence line) is an unequivocal demonstration of the impacts from an individual event be it idling, taxiing, takeoff run up, or landing. Nonetheless, it is equally important to track the impacts of dispersed plumes over the affected populations in an airport's vicinity.

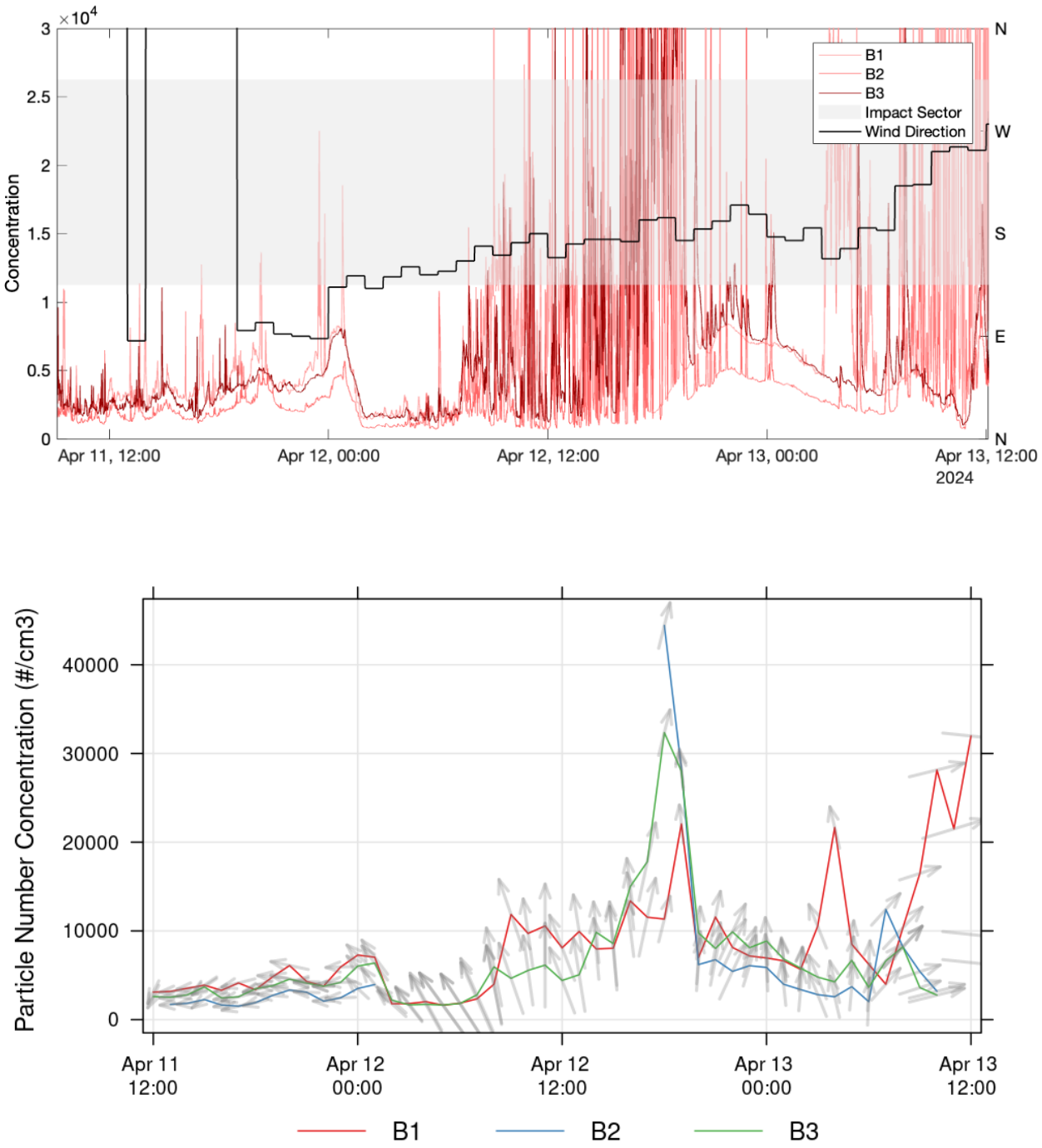

Figure 1.6 Particle number concentration (particles/cm^3) trends at three Bedford sites (B1 & B2: private residences and B3: Glenn Middle School) and surface wind at hourly average resolution. The upper and lower panels show different representations of the same data to facilitate interpretation: upper panel shows 1-second measurements while the lower panel shows the average of each hour of data.

1.3.4 Impacts on baseline air quality across neighborhoods

When emissions generated by aircraft and ground-based support vehicles at an airport disperse, it causes increases in baseline concentrations at sites downwind of the airport. When the wind changes direction and sites are no longer downwind of the airport, the concentrations decrease. We observed this pattern at all the sites in Bedford, Lincoln, and Concord.[6] Figure 1.6 shows data from the three Bedford sites and Figure 1.7 shows data from the two Concord sites; wind direction is shown on the secondary Y axis on the right-hand side of the figures. These figures illustrate that air quality can change rapidly depending on aviation activity and wind direction.

The following observations are noteworthy. Foremost, the same temporal pattern is observed at multiple sites (three sites in Bedford and two in Concord) including instances of spikes that are detected concurrently at multiple sites hundreds of feet apart. This suggests that the impact is from a wide-reaching source (as opposed to an idling or passing car, which would only impact one site) that is pervasive across the community. This was also reconfirmed by mobile monitoring where we observed higher concentrations over large areas (several square miles) downwind of the airport. We show four days of mobile monitoring data in Figure 1.8 for PNC and for nitrogen dioxide and black carbon in Figures 1.9 and 1.10, respectively. Additional mobile monitoring results are shown in Figure A.5 in the appendices.

1.3.5 Seasonal differences

We observed seasonal differences in PNC during the study, but the differences varied by site (Table 1.4). At M1, PNC was generally higher during the colder months than during the warm months. This trend has been observed in other studies in the Boston area (e.g., Padro-Martinez et al., 2012; Simon et al., 2016) and can be explained by differences in mixing height and dispersion between the two seasons (typically greater mixing heights and more dispersion in summer). At B1 and B2, the highest percentiles (95th) for PNC were higher in cold months than in the warm months (possibly reflecting short-lived aviation plumes (Chung et al., 2023)); however, the opposite was true for the average PNC, which was higher during the warm months than during cold months. One possible explanation for this is that both B1 and B2 are very close to runways (<500 m), and that may make PNC correlate more with emissions (i.e., flight activity), which are generally higher in the summer (Figure 1.1).

[6] Because the two Lexington sites were downwind of I-95 during westerly winds, we cannot rule out the highway as being the main source of ultrafine particles at these sites.

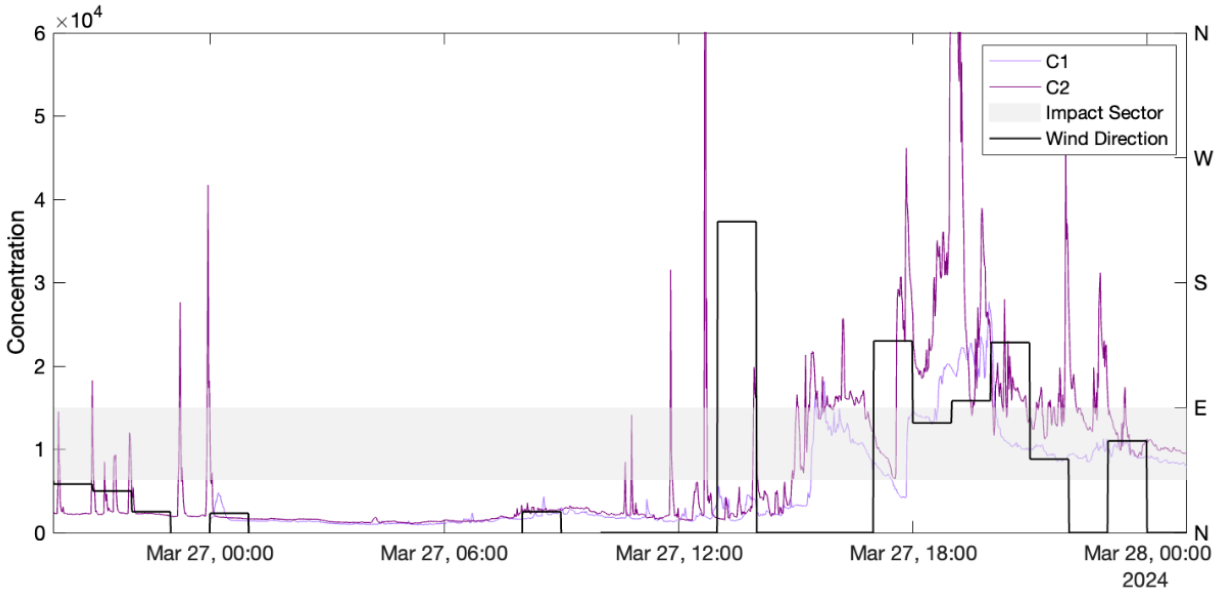

Figure 1.7 Particle number concentration (particles/cm^3) trends at two Concord sites (C1: a private residence and C2: Thoreau Farm) and surface wind direction at hourly average resolution.

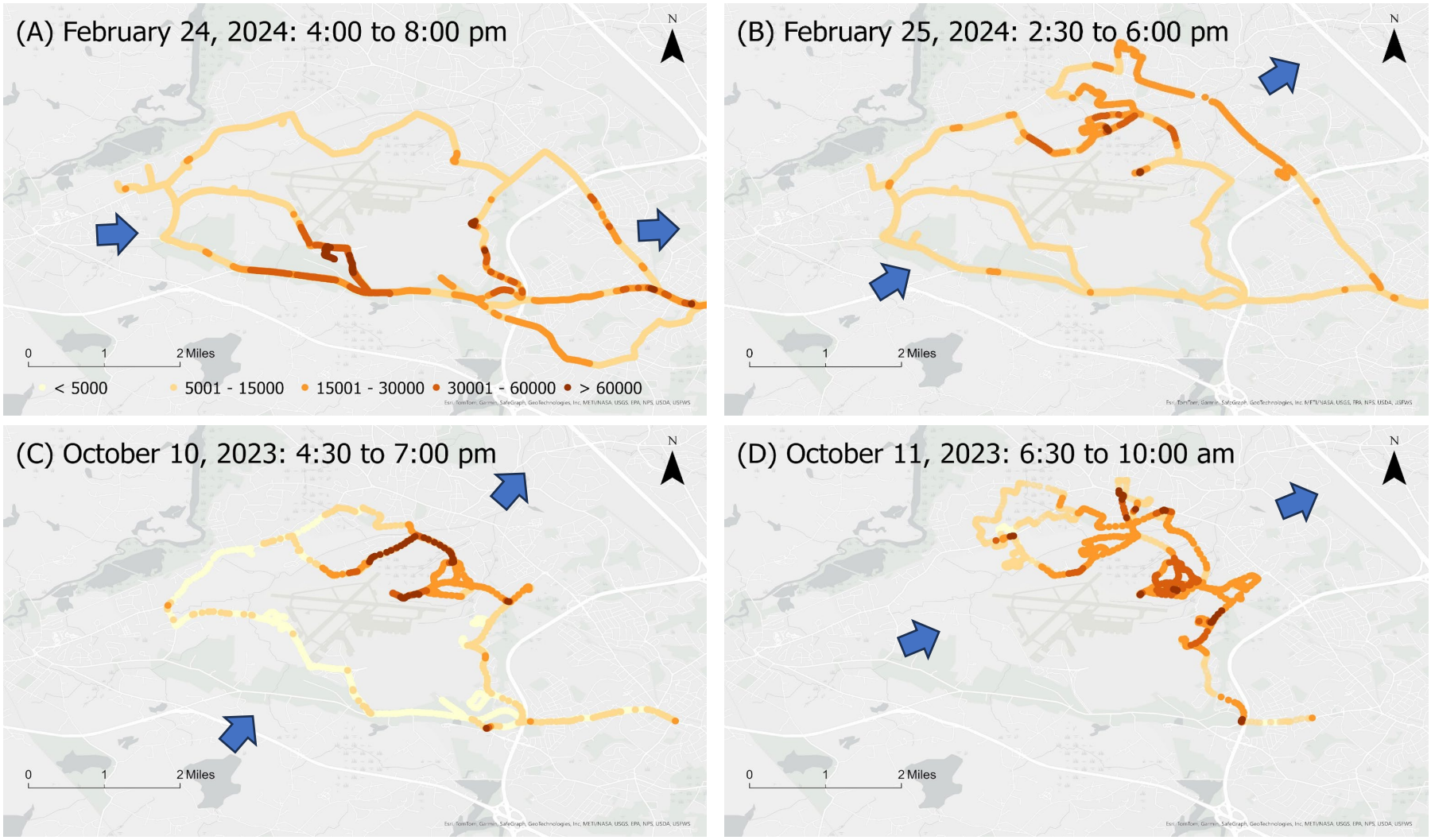

Figure 1.8 Spatial distribution of PNC (particles/cm^3) based on 1-second measurements made on two days of mobile monitoring in 2023 and two days in 2024.

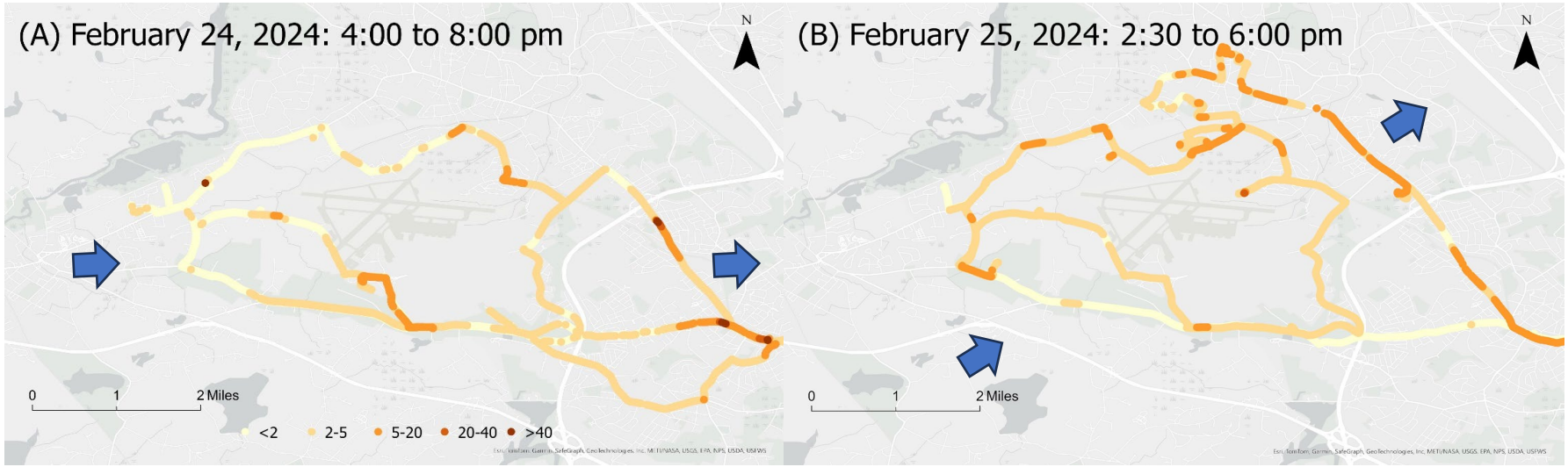

Figure 1.9 Spatial distribution of NO_2 (parts per billion) based on 10-second measurements made on two days of mobile monitoring in 2024.

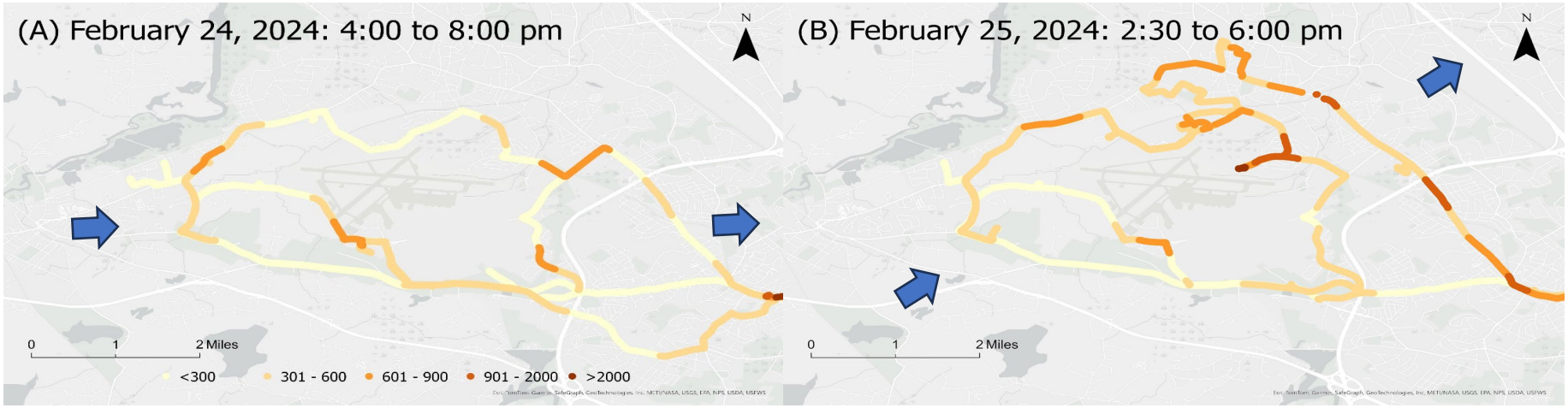

Figure 1.10 Spatial distribution of black carbon (ng/m^3) based on 1-minute measurements made on two days of mobile monitoring in 2024.

Table 1.4 Summary statistics for PNC for sites where measurements were made in two seasons.

Site	Season	Calm		Impact Sector		Non-Impact Sector	
		Mean (stdev)	Median (iqr)	Mean (stdev)	Median (iqr)	Mean (stdev)	Median (iqr)
B1	Cold	14400 (9100)	11800 (8900)	8300 (9000)	4600 (8500)	6300 (4700)	4800 (5100)
B1	Warm	8100 (5700)	6100 (8900)	9700 (8400)	7300 (7800)	7200 (5900)	5400 (5000)
B2	Cold	6300 (3500)	5700 (4100)	6800 (5800)	5100 (5000)	4400 (3200)	3500 (3600)
B2	Warm	9300 (NA)[1]	9300 (NA)[1]	11100 (4700)	9800 (8000)	5000 (3400)	4200 (3500)
M1	Cold	7000 (3600)	6000 (3600)	8300 (6500)	7400 (5400)	5900 (4300)	4800 (4700)
M1	Warm	4700 (2800)	4100 (1400)	6300 (3500)	5500 (5000)	4900 (3300)	4000 (2900)

Stdev = standard deviation
Iqr = interquartile range
[1]There was only one hour of calm wind during the warm-weather monitoring period at B2; thus, the standard deviation and interquartile range were not calculated.

As seen in Figures 1.11 and 1.12 and Table 1.4 in both seasons the highest PN concentrations occurred when the sites were directly downwind of the airfield (i.e., in the airport impact sector). The greater spread of the points in the PNC polar plots in colder months reflects generally higher wind speeds during colder months as compared to warmer months.

1.3.6 Exceedance of WHO guideline thresholds

Our measurements indicate that in the vicinity of Hanscom Field UFP concentrations always exceeded the WHO's low threshold 24-hour mean (1,000 particles/cm^3) and often exceeded the high threshold 24-hour mean (>10,000 particles/cm^3) and the high threshold 1-hour mean (20,000 particles/cm^3) (Table 1.5). The high threshold exceedances occurred more often when sites were downwind of the airport. The bullet points below describe the exceedances.

- At Thoreau Farm in Concord (site C2; ~0.4 miles from the airport), ultrafine particle number concentration (PNC) exceeded the high threshold 24-hour mean 77% of the time and the high threshold 1-hour mean 24% of the time when the site was downwind of the airport. In contrast, these exceedances were observed only 18% and 5% of the time, respectively, when the site was not downwind of the airport.
- At the Minuteman National Historic Park site in Lincoln (site M1; ~0.7 miles from the airport), PNC exceeded the high threshold 24-hour mean 31% of the time and the high threshold 1-hour mean 3% of the time when the site was downwind of the airport. When the site was not downwind of the airport, these exceedances were observed only 5% and 1% of the time, respectively.

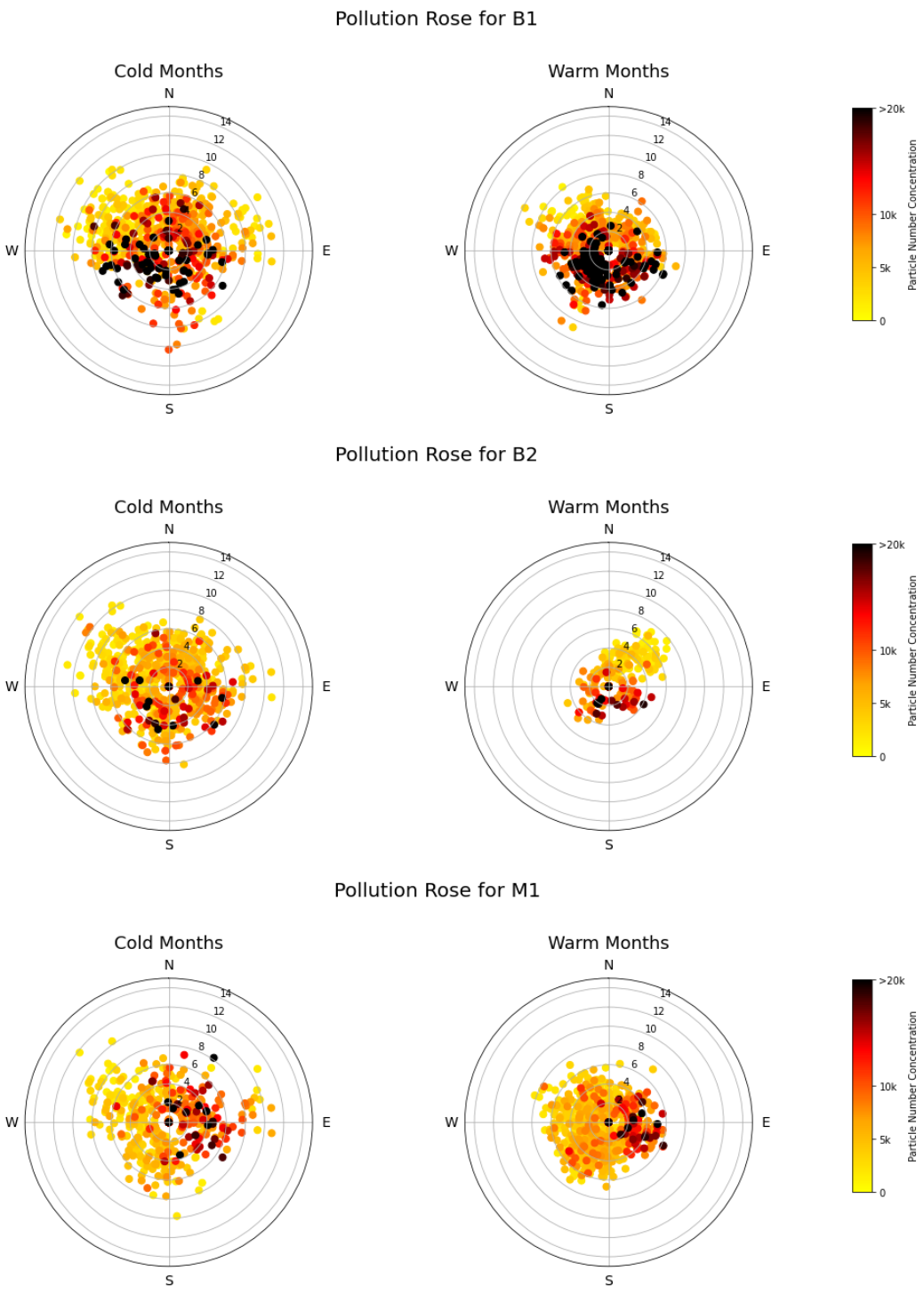

Figure 1.11 PNC polar plots comparing cold weather and warm weather monitoring for three sites near Hanscom Field. Each dot represents the average of 1-hour of data; the color of each dot is proportional to the hourly averaged concentration (particles/cm^3).

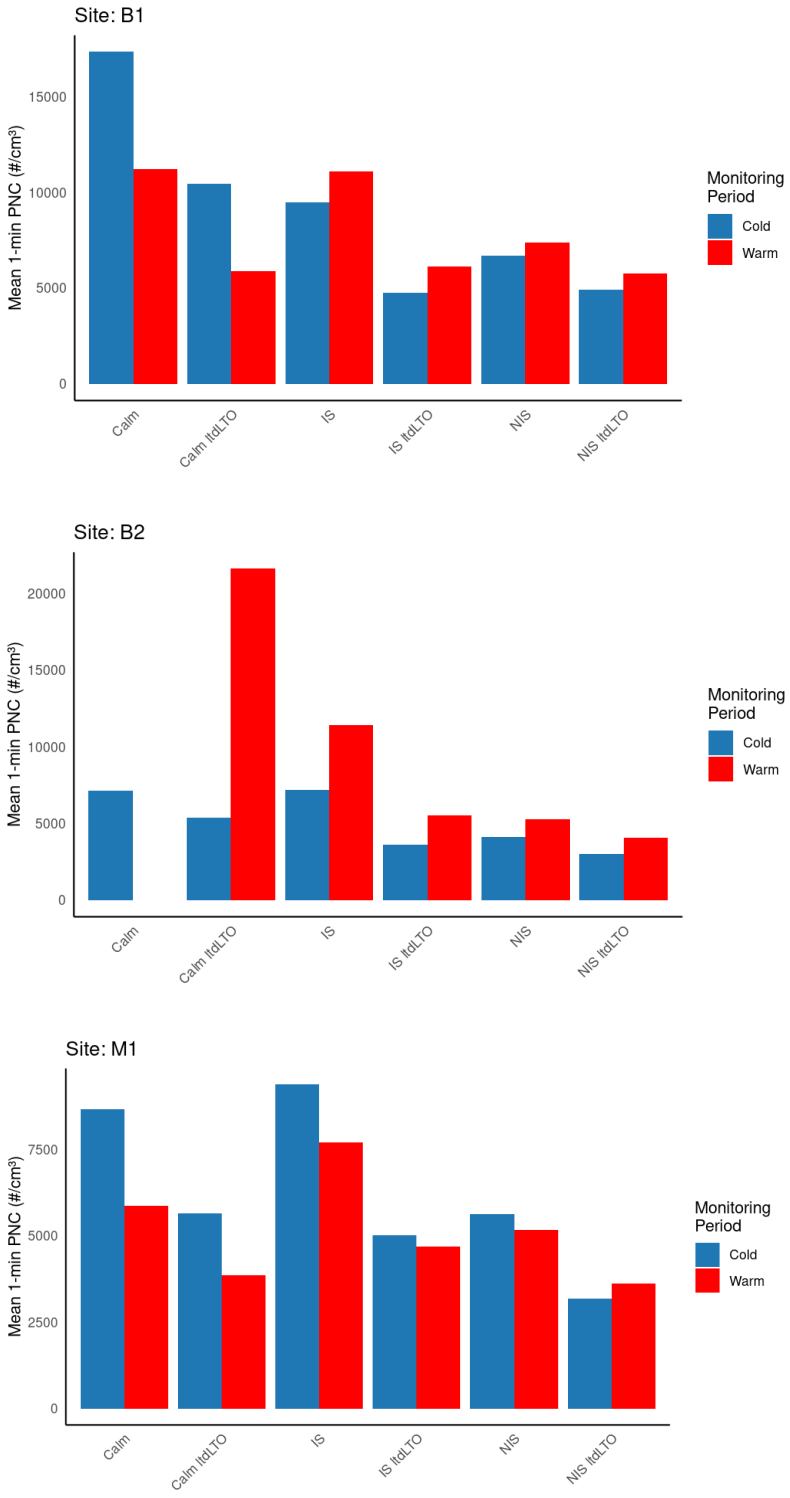

Figure 1.12 Bar charts showing mean 1-minute particle number concentrations for cold and warm months at two sites in Bedford and one in Lincoln. Calm = winds <0.5 m/s; IS = impact sector; NIS = non-impact sector; LTO = total number of landings and takeoffs; ltdLTO = limited landings and takeoffs during airport quiet hours (2300-0700).

Table 1.5 PNC exceedances of WHO UFP guidelines by site and wind conditions. Numbers indicate % of days/hours of monitoring that daily/hourly average UFP concentration exceeded the relevant guideline.

Site	All winds		Calm		Impact sector		Non-impact sector	
	24-h	1-h	24-h	1-h	24-h	1-h	24-h	1-h
B1	32%	8%	43%	11%	33%	1%	29%	3%
B2	6	1	7	1	16	3	4	0
B3	8	2	1	4	0	7	9	1
C1	6	1	2	0	6	0	4	2
C2	25	7	26	3	79	27	18	5
M1	4	1	1	2	15	2	3	1
L1	19	2	4	7	0	2	14	0
L2	1	0	1	2	0	0	1	0
B1 butanol[1]	42	1	76	24	32	12	36	4

24-h guideline = PNC is considered to be "high" if 24-h mean is >10,000 particles/cm^3.
1-h guideline = PNC is considered to be "high" if 1-h mean is >20,000 particles/cm^3.
[1]Based on a butanol CPC (TSI model 3775), which has a lower particle size cutoff (~4 nm) compared to the other CPC (TSI model 3783) also used at this and all other sites.

- At the residential site in Bedford very close to the airport (site B1), PNC exceeded the high threshold 24-hour mean 32% of the time and the high threshold 1-hour mean 12% of the time when the site was downwind of the airport. When the site was not downwind of the airport, these exceedances were observed for 36% and 4% of the time, respectively. During calm conditions PNC exceeded the high threshold 24-hour mean 76% of the time and the high threshold 1-hour mean 24% of the time; however, it is important to note that under calm conditions the site is more impacted by sources in the immediate vicinity.
- At the John Glenn Middle School site in Bedford (site B3; ~1 mile from the airport), PNC exceeded the high threshold 1-hour mean 7% of the time when the site was downwind of the airport. When the site was not downwind of the airport, this exceedance was observed only 2% of the time.

These numbers are highly dependent on the number of observations in the data set; therefore, it is important to note that the number of exceedances would likely change (increase or decrease) with a longer-term dataset. Ideally, the study should be conducted for at least a full year to have more complete coverage of seasonal and finer-resolution meteorological conditions that impact concentrations. It is also important to note that the fraction of exceedances is highly dependent on the size cutoff of the ultrafine particle monitor employed in the study. For example, at all eight stationary sites we used water-based CPCs with a particle size cutoff of ~7 nm; however, at site B1 we also co-located a butanol-based CPC with a particle size cutoff of ~4 nm. Because fresh combustion emissions are typically enriched in smaller particles (i.e., in the 1-10 nm size range), we expect to see higher particle number concentrations and

higher percentages of WHO-guideline exceedances with the butanol-based CPC as compared to the water-based CPC. Indeed, this is what we observed in the data from site B1 as illustrated in Tables 1.2, 1.3, and 1.5.

1.4 Summary and Conclusions

We monitored aviation-related air pollution markers in the four towns that abut Hanscom Field to develop a better understanding of the temporal and spatial distribution of pollutants near the airport. In two campaigns, including a cold-weather campaign between February 6 and April 28, 2024 and a warm weather campaign between July 12 and October 31, 2024, we measured UFP - a marker of aviation emissions - at eight stationary monitoring sites in the four towns for 27-112 days per site. At each site we collected data at 1-second intervals for 24 hours a day continuously allowing us to amass a rich dataset showing the temporal variation of UFP at different locations outside the airfield. We also performed mobile monitoring in the four towns to map the spatial extent of pollutant dispersion (spreading) beyond the airfield fence line. Our results show that UFP generated by aviation-related activities are being blown by the wind off the airfield and into the surrounding communities. In many instances there were substantial increases in pollutant concentrations at sites downwind of the airport relative to upwind sites. Also, at several sites, the UFP levels exceeded World Health Organization guidelines for good air quality.

While our study addressed many data gaps related to the impacts of Hanscom Airfield on air quality in surrounding communities, several other data gaps remain. For example, we did not perform any indoor air quality monitoring in homes near the airfield. In previous studies of air quality inside homes near airports (e.g., Boston Logan Airport (Hudda et al., 2020)), it has been shown that UFP from aviation activities can penetrate indoors and cause substantial increases in indoor concentrations. In future studies, it would be useful to measure UFP concentrations for 2-4 weeks in different seasons inside homes near Hanscom to better characterize infiltration and indoor exposures. Also, we did not have access to detailed flight activity data during the monitoring period; therefore, we were unable to investigate the impacts of specific types of aircraft and LTO patterns (e.g., frequency, time of day, runway usage) on air quality. In future studies it would be useful to obtain and analyze flight activity for the purposes of developing a better understanding of which types of aircraft and airfield operations are causing the greatest impacts on air quality. Such insights could be helpful for informing mitigation strategies.

2.0 Analysis of lead and other elements in $PM_{2.5}$ samples

2.1 Introduction

PM2.5 refers to airborne particles with a diameter less than 2.5 micrometers (um), which is approximately 30 times smaller than the diameter of a human hair. Due to their small size, PM2.5 particles can — like ultrafine particles (UFP) — penetrate deep into the lungs and enter the bloodstream. Exposure to UFP is associated with respiratory and cardiovascular diseases and with adverse developmental and neurological outcomes (Moreno-Ríos et al., 2022; Ohlwein et al., 2019; Schraufnagel, 2020). One important difference between PM2.5 and UFP is that PM2.5 concentrations are regulated under the Clean Air Act, whereas there are currently no established air quality criteria for UFP in the U.S.

PM2.5 is made up of complex mixtures of organic compounds, inorganic salts, and trace metals, often varying by source and location. This diversity reflects contributions from natural sources, such as soil, pollen, and dust, and anthropogenic activities, including fossil fuel combustion and industrial emissions. The composition of PM2.5 can influence its toxicity and health impacts (Bell, 2012), making its study critical for understanding and mitigating its risks to human health.

Hanscom Field is a general aviation airport that primarily serves non-commercial aircraft, including piston-engine planes. Piston-engine aircraft consume leaded aviation gasoline (avgas), which remains the only leaded fuel still in widespread use in the United States. Despite the phase-out of leaded gasoline for automobiles decades ago, avgas continues to be a significant source of airborne lead pollution. Piston-engine aircraft using leaded avgas account for nearly half of the airborne lead (Pb) emissions in the U.S. (U.S. EPA 2017). Lead is a potent neurotoxin, particularly harmful to children, as it can impair cognitive development and cause a range of health issues even at low exposure levels (Needleman and Bellinger 1991). Airports like Hanscom Field represent localized hotspots for lead emissions, underscoring the need to monitor and quantify lead exposure in surrounding communities.

2.1.1 Objectives

Our objectives were to

1. Collect and analyze particulate matter samples from across the airfield for a suite of elements including lead, bromine, sulfur, and arsenic as well as elements considered to be indicators of traffic-related emissions and common crustal elements;
2. Compare elemental composition among the Hanscom sites as well as between the Hanscom sites and the EPA Chemical Speciation Network site in Boston to identify possible patterns indicative of aviation emissions.

2.2 Methods

PM2.5 sampling equipment was co-located at four of the UFP monitoring sites (i.e., Minuteman National Park in Lincoln (M1); Thoreau Farm in Concord (C2); and two residential sites in Bedford (B1 and B2) (Figure 1.2)) from July 26 to September 24, 2024. We used both single-stage Harvard Personal Exposure Monitor (HPEM) and multi-stage Sioutas Personal Cascade Impactors (PCIS) to collect bulk particles <2.5 um and specific size distributions of particles (10 >x>2.5 um, 2.5>x>0.25 um, <0.25 um), respectively. The equipment was housed in temperature-controlled, weather-resistant shelters. Time-integrated PM2.5 samples were collected on PTFE filters for metals analysis. Filters were analyzed via gravimetry (40 CFR 50 Appendix L) and energy dispersive X-ray fluorescence spectrometry (XRF; U.S. EPA IO-3.3) at Alliance Technical Group (Tigard, OR). Samples were collected between 7-14 days for both HPEM and PCIS samplers. We used two sets of identical HPEM and PCIS samplers, rotating the samplers between the four sites to maximize the number of samples per site during the two-month campaign.

XRF was used to measure 38 elements from sodium (Na) to lead (Pb). Elements with >90% non-detects were excluded from analysis including (Figure 2.1). Instrument detection limits (DL) differed by element and by sample (e.g., different mass per sample), where measurements below detection limits were replaced with 0.5*DL. Lead was measured above instrument detection limits in 100% of samples (excluding field blanks) at all the sites. Lead concentrations in field blanks were below detection limits for >75% of samples; only the first PCIS chamber (measuring coarse particulate matter i.e., 10>x>2.5 um) of field blanks contained lead above the minimum detection limit and these measurements were small relative to experimental measurements (3-4-fold lower concentrations). No adjustments were made to account for these

Table 2.1 Particulate matter sampling dates and numbers of samples collected at each site.

Site	Dates (in 2024)	# Samples	HPEM (PM2.5)		PCIS (size-fractionated PM)[1]
			XRF (field blanks)	OC/EC (field blanks)[2]	XRF (field blanks)
B1	7/26 - 8/20	6	3	1	2
B2	8/20 - 9/24	7	3 (1)	2 (1)	2 (1)
M1	7/26 - 8/13	4	3	0	1
C2	8/13 - 9/24	9	4 (1)	3 (1)	2 (1)

[1]Includes quasi-UFP (<0.25 um), accumulation mode (2.5>x>0.25 um) and coarse mode (10 >x>2.5 um) PM fractions.
[2]Not chemically analyzed as part of this study.

differences because they were *de minimis*. In addition to lead, other elements including S, Cu, Fe, Zn, and Br, many of which are present in transportation emissions, were detected in 100% of the samples.

Measurements at the four sites were compared to data from the U.S. Environmental Protection Agency (EPA) Chemical Speciation Network (CSN) site in Boston (Site ID: 0042), which measures PM2.5 mass and elemental concentrations using similar protocols (EPA, 2025). CSN data from July to September 2024 were used as a reference to assess sample enrichment by comparing element concentrations relative to predominantly crustal elements (Si, Al, Ca, K) (Hudda et al., 2022). Although the Boston site is in a dense urban environment with a variety of local emission sources, including traffic, a nearby bus depot, construction projects, it is not influenced by emissions from piston-engine aircraft and is considered an urban background site.

2.2.1 Quality Assurance

Sites were serviced every 2-3 days to ensure air flow measurements were within manufacturer specification (10 liters/min for HPEM and 9 liters/min for PCIS), and the samplers were cleaned between deployments. Blanks were collected at a rate of 23% (6 blanks per 26 actual samples) to quantify sampling errors. Co-located HPEM instruments produced consistent results, with mass measurements differing by less than 2%.

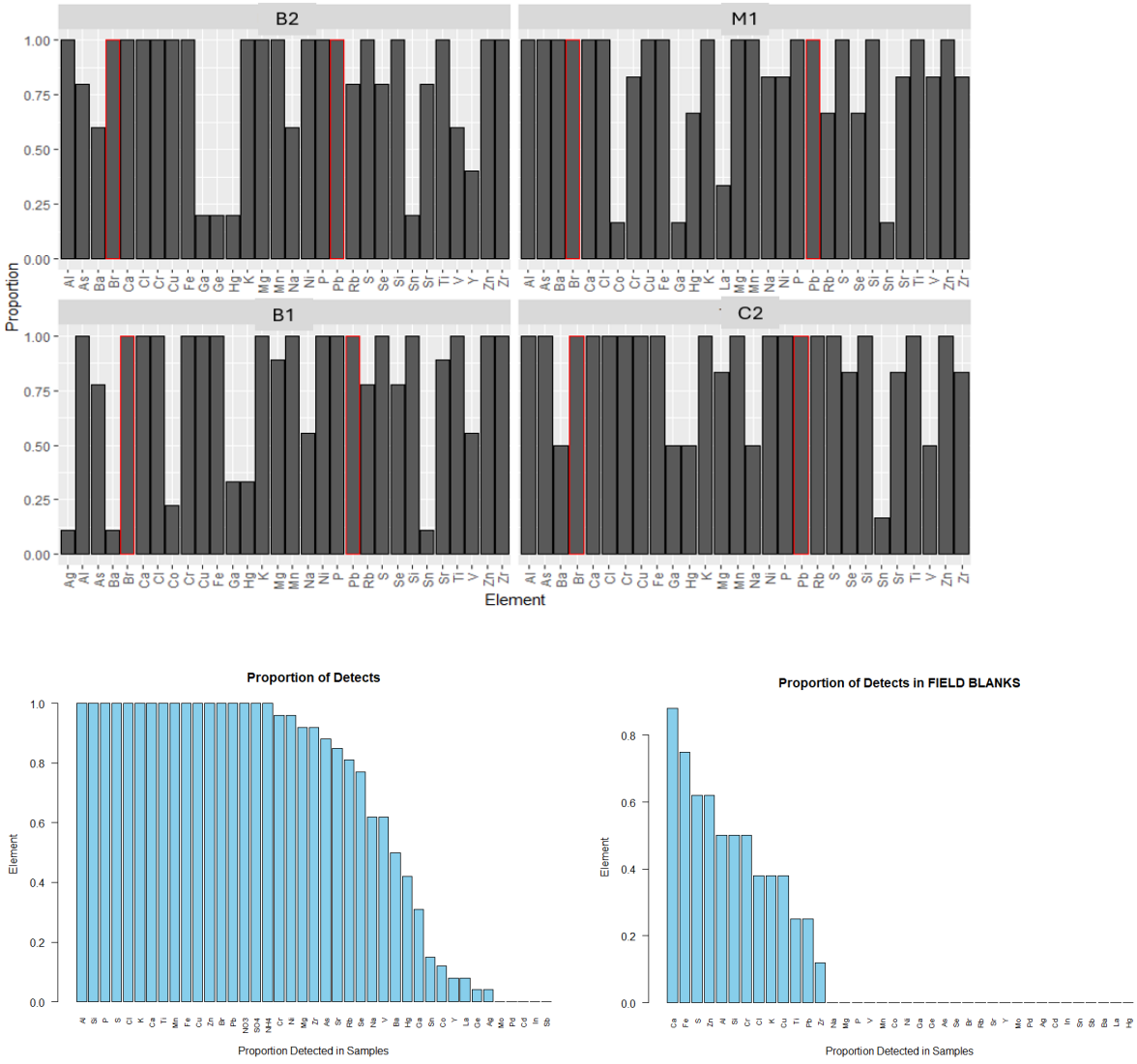

Figure 2.1 (Upper panel) Proportions of detections by element and monitoring site, (lower left panel) proportion of detects across all sites, and (lower right panel) proportion of detects in field blanks. The following elements were excluded from analysis because they were not detected in >90% of the samples: Y, Pd, Ag, Cd, In, Sb, Ge, Mo, Co, and La.

2.3 Results and Discussion

2.3.1 Time-integrated PM2.5 mass and size distribution measurements

The highest PM2.5 mass concentrations were measured at B1 and C2, the sites located closest to Hanscom Field (Table 2.2). Additionally, mean PM2.5 concentrations at B1 and C2 exceeded the average

concentration at the CSN site in Boston during the same period (July to September 2024); however, differences in sample collection times (7-14 days/sample at Hanscom vs. 1 day/sample at the CSN site) and the number of samples collected (n=2 at Hanscom vs. n=36 at the CSN site) suggest that the differences in PM2.5 concentrations measured at the two locations are not likely to be statically significant. As expected for PM2.5, which is relatively spatially homogeneous compared to UFP, there was relatively little variation in concentrations (≤25-33%) between concurrent samples collected across the airfield (Figure 2.2).

Particle size distributions varied by site: B1 and B2 showed peak mass in the <0.25 um (quasi-ultrafine) fraction, while M1 and C2 had the highest mass in the coarse fraction (10 >x>2.5 um) (Table 2.2; Figure 2.2). Although the PCIS has been validated in both laboratory (McMurray et al., 2002) and field (Singh et al., 2003) settings, it may underestimate coarse mode mass due to wall losses in the upper impactor stages (Berlinger et al. 2021). In contrast, quasi-ultrafine mass (<0.25 um) has shown stronger agreement with reference instruments and was highest at the sites closest to Hanscom Field. This is consistent with prior research showing that particles from piston-engine aircraft exhaust contain a higher fraction of ultrafine particles than other typical sources - e.g., ground-based motor vehicles (Griffith 2020).

2.3.2 Lead (Pb) concentrations

Mean lead (Pb) concentrations in PM2.5 samples at the four Hanscom sites were similar to one another based both on mass per volume of air (1.6 to 2.2 ng/m^3) and on mass per mass of particles (0.19 to 0.31 ng/ug) (Table 2.3)[7]. In addition, mean Pb concentrations in PM2.5 samples at the four sites were similar to Pb concentrations at the CSN site in Boston in terms of mass per volume of air, but not in terms of mass per mass of particles: the mean mass concentration of Pb at the Boston site was 0.45 ng/ug, roughly 2-fold higher than at the Hanscom sites. In addition, Pb-to-Br mass concentration ratios were between 0.79 and 1.1 at the Hanscom sites, while at the Boston CSN site the same ratio was ~7-fold higher. Taken together, these results suggest that the source of Pb at Hanscom is different from that in Boston. Furthermore, the elevated Br concentrations we observed at the Hanscom sites are consistent with aviation-related emissions (Griffith 2020): ethylene dibromide ($C_2H_4Br_2$) is added to leaded aviation gasoline to scavenge Pb during combustion and thereby prevent engine fouling; thus, this may explain the relatively elevated Br concentrations we observed at the near-airport sites. Based on analysis of the PCIS samples, the highest fraction of Pb was found the quasi-UFP fraction in all samples (Figure 2.3).

[7] The National Ambient Air Quality Standard for lead is 150 ng/m^3 based on a 3-month average.

Table 2.2 Mean particle mass concentrations.

Site	HPEM <2.5 um (ug/m^3)	PCIS 10>x>2.5 um (ug/m^3)	PCIS 2.5>x>0.25 um (ug/m^3)	PCIS <0.25 um (ug/m^3)	Sum PCIS <10 um (ug/m^3)	MassDEP reconstructed mass PM2.5 LC (ug/m^3)[1,2]
B1	12.4 (n=3)	3.7	5.1	5.5	14.3 (n=2)	
B2	7.2 (n=2)	3.0	2.3	3.7	9.0 (n=1)	
M1	9.1 (n=3)	3.2	1.5	2.1	6.8 (n=1)	
C2	12.4 (n=3)	3.4	2.2	3.2	8.8 (n=1)	
Boston (EPA CSN)						5.2 +/- 2.5 (n=29)

[1]Mass is calculated by summing weights of all the chemical species analyzed in the samples. LC = local conditions.
[2]MADEP 24hr time-integrated filter PM2.5 from 7/2/2024 - 9/21/2024 mean was 8.28 +/- 3.36 ug/m^3 (n=28 filter samples). This was measured using a Federal Reference Method monitor.

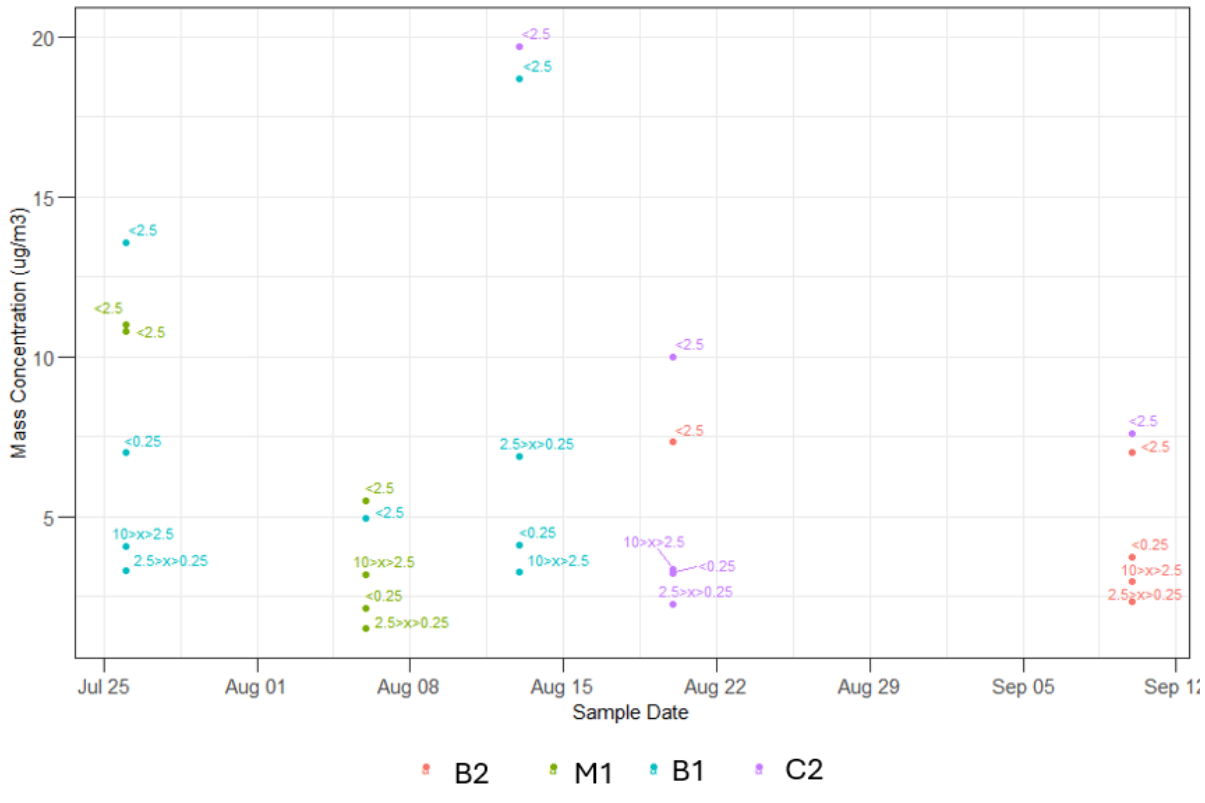

Figure 2.2 PM mass concentration by sample date and site.

2.3.3 Other elements

Across the Hanscom sites and the Boston EPA CSN site, lead (Pb) concentrations scaled similarly with crustal (Al, Si, Ca, K) and traffic-related (Fe, Cu, Zn) elements (Figure 2.4), indicating that Pb covaries with these markers across both environments, even though the dominant emission sources are different. Whereas the urban CSN site is characterized by street traffic, emissions from a bus depot, and construction activities, the Hanscom area sites experience only intermittent emissions associated with mainly jet engine aircraft (89% Jet-engine, 11% piston-engine aircraft; FAA TFMSC, 2025), which do not use leaded avgas. As shown in Figure 2.4 and consistent with findings from Section 2.3.2, Hanscom samples exhibited elevated Br concentrations relative to Pb compared with the Boston site, indicating that the additional Pb in the Hanscom samples is due to a source on or nearby Hanscom airfield – most likely avgas. Thus, while the proportional relationships between Pb and crustal or traffic tracer elements appear regionally consistent, the Pb-to-Br ratio strongly suggests a unique contribution of piston-engine aircraft emissions at Hanscom Field.

Table 2.3 Concentrations of Pb, Br, As, and S in time-integrated PM samples[1].

Site	Sample Size (number of non-duplicate samples)[2]	Pb		Br		As		S	
		ng/m^3	ng/ug	ng/m^3	ng/ug	ng/m^3	ng/ug	ng/m^3	ng/ug
B1	2	2.21 (0.39)	0.26 (0.18)	2.99 (0.80)	0.24 (0.071)	0.51 (0.08)	0.044 (0.015)	253 (77.5)	24.0 (10.1)
B2	2	2.19 (0.61)	0.31 (0.13)	2.41 (0.11)	0.34 (0.11)	0.67 (0.07)	0.092 (0.011)	231 (6.9)	32.3 (1.97)
M1	2	1.57 (0.22)	0.19 (0.047)	1.93 (0.51)	0.24 (0.020)	0.58 (0.14)	0.071 (0.008)	251 (62.6)	28.4 (3.63)
C2	3	2.25 (0.67)	0.23 (0.15)	2.66 (0.70)	0.24 (0.088)	0.71 (0.15)	0.072 (0.043)	268 (68.9)	24.0 (9.21)
Boston (EPA CSN)[3]	29	2.1 (4.7)	0.45 (0.75)	0.20 (0.51)	0.059 (0.12)	ND[4]	ND[5]	245 (141)	45.4 (17.8)

[1]Reported here as the mean and standard deviation (in parentheses) in ng of element/m^{3}of air and ng of element/ug of particles.

[2]Sample size denotes independent samples. Results from duplicate co-located samples were first averaged and then averaged with the other independent samples to avoid biasing results.

[3]Samples were collected between July and September 2024. Mass/mass concentrations were based on reconstructed PM2.5 mass concentrations (see Table 2.2).

[4]ND = not detected. The minimum detection limit for As in terms of mass/volume was 1.2 ng/m^3 (EPA, 2025)

[5]Minimum detection limit for As in terms of mass/mass of particles was not reported.

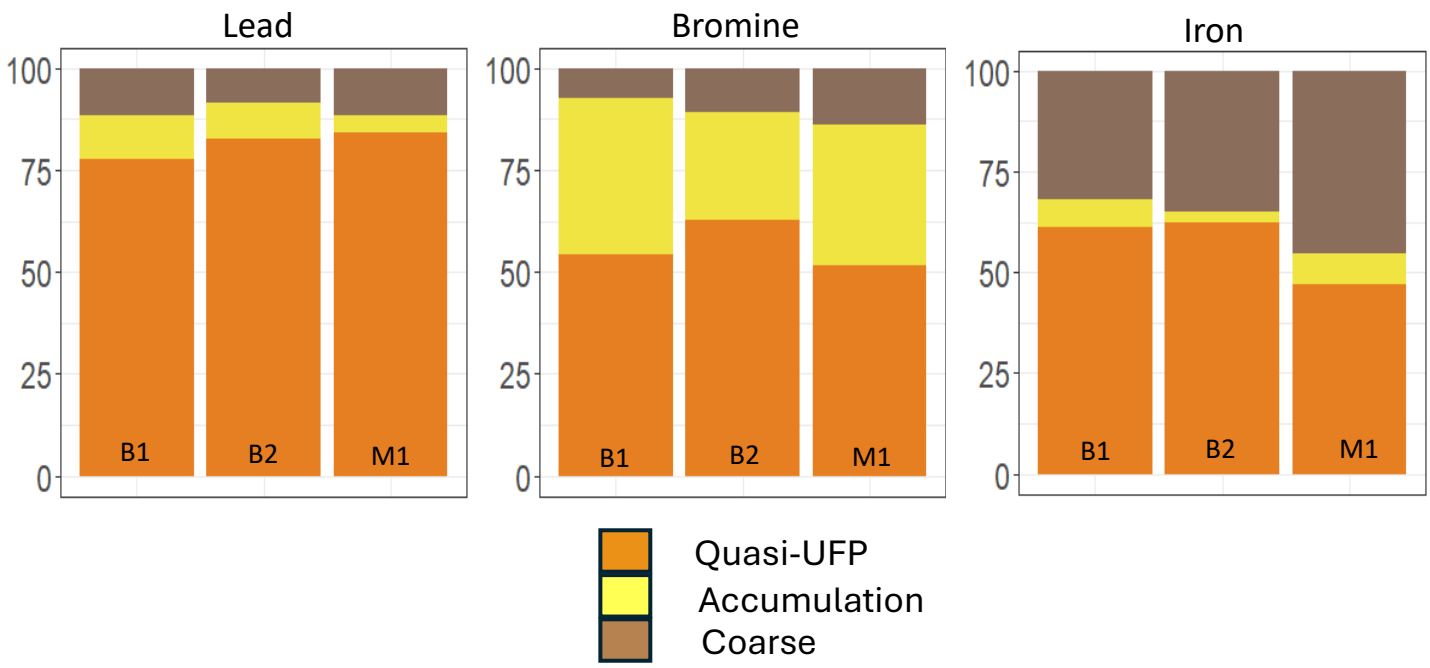

Figure 2.3 Percentage of Pb, Br, and Fe content by particle size at three monitoring sites near Hanscom. Results from C2 are not presented due to sampler error.

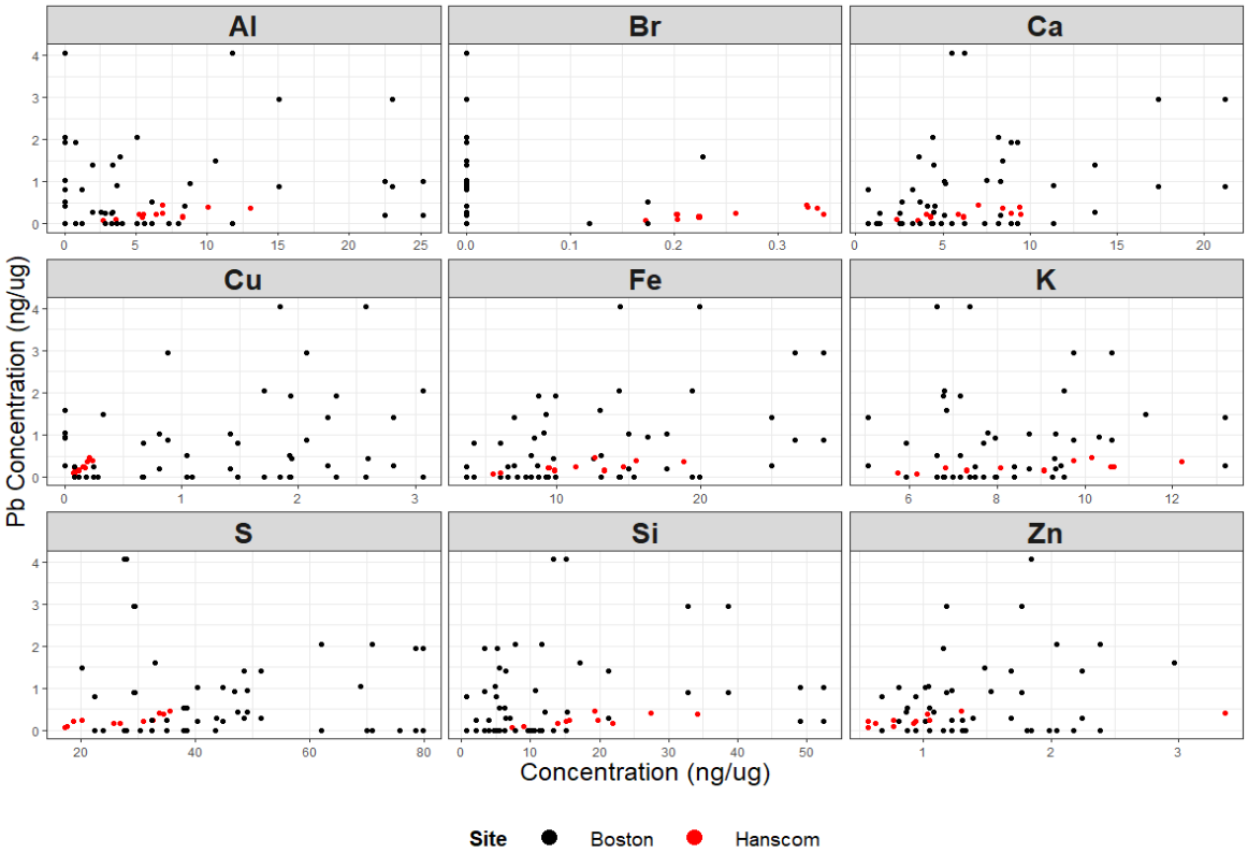

Figure 2.4 Concentrations of airborne Pb versus other elements in the Hanscom samples (n=9) and in samples from the EPA Chemical Speciation Network (CSN) site in Boston (n=29) during the study period. Hanscom mass element per mass total PM2.5 concentrations are indicated in red, while CSN mass element per mass Reconstructed PM2.5 concentrations are in black.

2.4 Summary and Conclusions

Between July and September 2024, we collected time-integrated PM samples at four sites near Hanscom Field to investigate the potential impacts of aviation-related emissions on PM2.5 mass concentrations, ambient lead, and other elements of interest.

Key findings include the following:

- PM2.5 mass concentrations were highest at sites closest to the airfield.
- There was no difference in ambient lead concentrations across the four sites and all measurements were much lower than National Ambient Air Quality Standards.
- In size segregated PM samples, the highest lead concentrations were found in the smallest particle size fraction (i.e., quasi-ultrafine fraction, <0.25 um), consistent with emissions from aircraft activity near general aviation airports.
- The concentrations of bromine, a known tracer of aviation gasoline, at all four sites were much higher than at a reference site in Boston, providing further evidence of near-field aviation impacts.

Taken together, these findings indicate that aviation activities at Hanscom Field are impacting PM2.5, lead and bromine concentrations in areas outside the airfield. While our small sample size did not allow for robust statistical analysis or for detailed source apportionment of PM2.5 and lead, our results provide a useful baseline dataset against which plans increased aviation activity at the airfield could be evaluated.

3.0 References

Austin, E. et al. (2021). Distinct Ultrafine Particle Profiles Associated with Aircraft and Roadway Traffic. Environmental Science & Technology, 55, 2847–2858.

Babisch, W., Kamp, I. (2009). Exposure-response relationship of the association between aircraft noise and the risk of hypertension. Noise & Health, 11, 161.

Bell ML, HEI Health Review Committee (2012) Assessment of the health impacts of particulate matter characteristics. Research Report (Health Effects Institute). (161):5-38. PMID: 22393584.

Code of Federal Regulations, 40 CFR 50 Appendix L, Reference method for the determination of fine particulate matter as PM2.5 in the atmosphere, https://www.ecfr.gov/current/title-40/chapter-I/subchapter-C/part-50/appendix-Appendix%20L%20to%20Part%2050.

Correia, A. W., Peters, J. L., Levy, J. I., Melly, S., Dominici, F. (2013). Residential exposure to aircraft noise and hospital admissions for cardiovascular diseases: multi-airport retrospective study. BMJ 347, f5561.

Dimakopoulou, K. et al. (2017). Is aircraft noise exposure associated with cardiovascular disease and hypertension? Results from a cohort study in Athens, Greece. Occupational & Environmental Medicine, 74, 830–837.

Eagan, M. E., Nicholas, B., McIntosh, S., Clark, C., Evans, G. (2017). Assessing Aircraft Noise Conditions Affecting Student Learning–Case Studies. ACRP Web-Only Doc.

Franssen, E. A. M., van Wiechen, C. M. A. G., Nagelkerke, N. J. D., Lebret, E. (2004). Aircraft noise around a large international airport and its impact on general health and medication use. Occupational & Environmental Medicine, 61, 405–13.

Fritz S, Aust S, Sauter T (2022) Impact of the closure of Berlin-Tegel Airport on ultrafine particle number concentrations on the airfield, Frontiers in Environmental Science, 10–2022, https://www.frontiersin.org/journals/environmental-science/articles/10.3389/fenvs.2022.1061584, DOI=10.3389/fenvs.2022.1061584z.

Griffith, 2020. Electron microscopic characterization of exhaust particles containing lead dibromide beads expelled from aircraft burning leaded gasoline. *Atmospheric Pollution Research* 11:1481-1486.

Habre, R. et al. (2018). Short-term effects of airport-associated ultrafine particle exposure on lung function and inflammation in adults with asthma. Environ. Int. 118, 48–59.

HEI (2013). Understanding the health effects of ambient ultrafine particles. HEI Review Panel on Ultrafine Particles. Boston (MA): Health Effects Institute.

Hsu H-H, Adamkiewicz G, Houseman EA, Vallarino J, Melly SJ, Wayson RL, Spengler JD, Levy JI (2012) The relationship between aviation activities and ultrafine particulate matter concentrations near a mid-sized airport, Atmospheric Environment, 50, 328-337, https://doi.org/10.1016/j.atmosenv.2011.12.002.

Hudda N, Fruin S, Durant JL (2022) Substantial near-field air quality improvements at a general aviation airport following a runway shortening, Environmental Science & Technology, https://doi.org/10.1021/acs.est.1c06765.

Hudda N, Simon MC, Patton AP, Durant, JL (2020a) Air quality improvements in a near-highway urban neighborhood during the COVID-19 pandemic, Science of the Total Environment, https://doi.org/10.1016/j.scitotenv.2020.140931.

Hudda N, Durant LW, Fruin S, Durant JL (2020b) Infiltration of aviation-related ultrafine particles inside a residence near an airport, Environmental Science & Technology, https://dx.doi.org/10.1021/acs.est.0c01859.

Hudda, N., Fruin, S. A. (2016). International Airport Impacts to Air Quality: Size and Related Properties of Large Increases in Ultrafine Particle Number Concentrations. Environmental Science & Technology, 50, 3362–3370.

Hudda, N., Gould, T., Hartin, K., Larson, T. V., Fruin, S. A. (2014). Emissions from an international airport increase particle number concentrations 4-fold at 10 km downwind. Environmental Science & Technology, 48, 6628–6635.

Hudda, N., Simon, M. C., Zamore, W., Brugge, D., Durant, J. L. (2016). Aviation Emissions Impact Ambient Ultrafine Particle Concentrations in the Greater Boston Area. Environmental Science & Technology, 50, 8514–8521.

Hudda, N., Simon, M. C., Zamore, W., Durant, J. L. (2018). Aviation-Related Impacts on Ultrafine Particle Number Concentrations Outside and Inside Residences near an Airport. Environmental Science & Technology, 52, 1765–1772.

Huss, A., Spoerri, A., Egger, M., Röösli, M., Swiss National Cohort Study Group (2010). Aircraft Noise, Air Pollution, and Mortality from Myocardial Infarction. Epidemiology 21, 829–836

Keuken, M.P., Moerman, M., Zandveld, P., Henzing, J.S., Hoek, G. (2015). Total and size-resolved particle number and black carbon concentrations in urban areas near Schiphol airport (the Netherlands), Atmospheric Environment, 104, 132-142.

Jarup, L. et al. (2008). Hypertension and Exposure to Noise Near Airports: the HYENA Study. Environmental Health Perspectives. 116, 329.

Lammers, A. et al. (2020). Effects of short-term exposures to ultrafine particles near an airport in healthy subjects. Environment International 141.

Lin, S. et al. (2008). Residential proximity to large airports and potential health impacts in New York State. Int. Arch. Occupational & Environmental Health, 81, 797–804.

Masiol, M., Harrison R.M. (2014). Aircraft engine exhaust emissions and other airport-related contributions to ambient air pollution: A review. Atmospheric Environment, 95, 409-455. http://dx.doi.org/10.1016/j.atmosenv.2014.05.070.

Matsui, T. et al., (2003). Association between the Rates of Low Birth Weight and/or Preterm Infants and Aircraft Noise Exposure. Nippon Eiseigaku Zasshi Japanese Journal of Hygiene, 58, 385–394.

Moreno-Ríos, A.L., Tejeda-Benítez, L.P., Bustillo-Lecompte, C.F. (2022). Sources, characteristics, toxicity, and control of ultrafine particles: An overview, Geoscience Frontiers, 13(1), 101147.

Needleman HL, Bellinger, D (1991). The health effects of low level exposure to lead, Annual Reviews of Public Health. 1991. 12:111-40.

Ohlwein, S., Kappeler, R., Kutlar Joss, M., Künzli, N., Hoffmann, B. (2019). Health effects of ultrafine particles: a systematic literature review update of epidemiological evidence, International Journal of Public Health, 64(4), 547-559.

Rosenlund, M., Berglind, N., Pershagen, G., Järup, L., Bluhm, G. (2001). Increased prevalence of hypertension in a population exposed to aircraft noise. Occupational & Environmental Medicine, 58, 769–73.

Schraufnagel, D.E. (2020). The health effects of ultrafine particles, Experimental & Molecular Medicine, 52, 11–317.szdx.

Simon MC, Hudda N, Naumova E, Levy JI, Brugge D, Durant JL. (2017) Comparisons of traffic-related ultrafine particle concentrations measured in two urban areas by central, residential, and mobile monitoring," Atmospheric Environment, 169, 113-127; DOI: 10.1016/j.atmosenv.2017.09.003.

Stacey, B. (2019). Measurement of ultrafine particles at airports: A review. Atmospheric Environment 198, 463–477.

Stacey, B., Harrison, RM, Pope F. (2020). Evaluation of ultrafine particles concentrations and size distributions at London Heathrow Airport, Atmospheric Environment, 222, 117148, https://doi.org/10.1016/j.atmosenv.2019.117148.

US EPA (1999), Method IO-3.3, DETERMINATION OF METALS IN AMBIENT PARTICULATE MATTER USING X-RAY FLUORESCENCE (XRF) SPECTROSCOPY, Center for Environmental Research Information, Office of Research and Development, U.S. Environmental Protection Agency, Cincinnati, OH 45268.

US EPA (2025). Chemical Speciation Network (CSN) Annual Quality Report: Samples Collected January 1, 2023 through December 31, 2023. Prepared by Air Quality Research Center, UC Davis.

US EPA (2023), Finding That Lead Emissions From Aircraft Engines That Operate on Leaded Fuel Cause or Contribute to Air Pollution That May Reasonably Be Anticipated To Endanger Public Health and Welfare, A Rule by the Environmental Protection Agency on 10/20/2023, https://www.federalregister.gov/documents/2023/10/20/2023-23247/finding-that-lead-emissions-from-aircraft-engines-that-operate-on-leaded-fuel-cause-or-contribute-to.

US EPA (2019a). Integrated Science Assessment (ISA) for particulate matter (final report, December 2019). Washington (DC): United States Environmental Protection Agency (EPA/600/R-19/188).

Wing, S. E. et al. (2020). Preterm Birth among Infants Exposed to In Utero Ultrafine Particles from Aircraft Emissions. EHP5732.

Wu, A. H. et al. (2021). Association between Airport-Related Ultrafine Particles and Risk of Malignant Brain Cancer: A Multiethnic Cohort Study. Cancer Research, 81, 4360–4369.

Appendices

Table A.1. Sample size (hours) by season and monitoring site.

Site	Cold Weather	Warm Weather
B1 (+butanol)	IS: 536 NIS: 725 Calm: 108	IS: 933 NIS: 457 Calm: 88
B2	IS: 140 NIS: 601 Calm: 143	IS: 44 NIS: 276 Calm: 1
B3	IS:41 NIS: 338 Calm: 82	IS: NA NIS: NA Calm: NA
C1l	IS: 55 NIS: 344 Calm: 86	IS: NA NIS: NA Calm: NA
C2	IS: 85 NIS: 736 Calm: 137	IS: NA NIS: NA Calm: NA
L1	IS:58 NIS:502 Calm:135	IS: NA NIS: NA Calm: NA
L2	IS:48 NIS:440 Calm:123	IS: NA NIS: NA Calm: NA
M1	IS: 54 NIS: 371 Calm: 97	IS: 60 NIS: 854 Calm: 74

IS = Impact sector winds
NIS = non-impact sector winds
Calm = wind speed was <0.5 m/s
NA = no monitoring was performed at this site during the warm weather months.

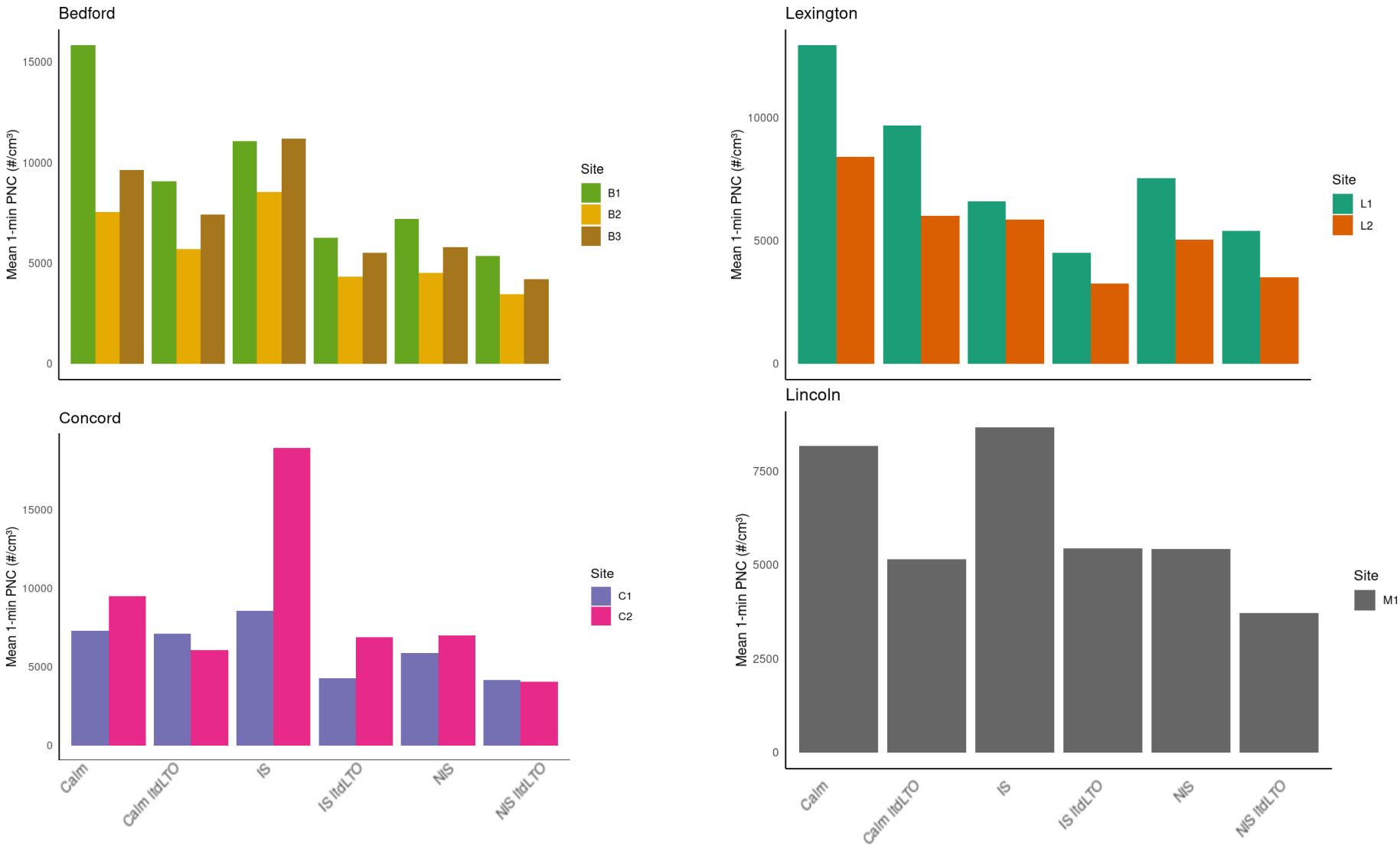

Figure A.1 Bar charts showing mean 1-minute PNC for various subsets of data. Length of bar indicates mean PNC for each subset. Data is binned by calm vs non-calm wind (wind speed >0.5 m/s). Non-calm hours are differentiated by whether the site was downwind of the airport (impact sector = IS) or not downwind of the airport (non-impact sector = NIS). Data is further split into periods of regular flight activity (LTO, landings and takeoffs), typically during the day (0700-2259), versus the night when there is limited (ltd) flight activity (2300-0659).

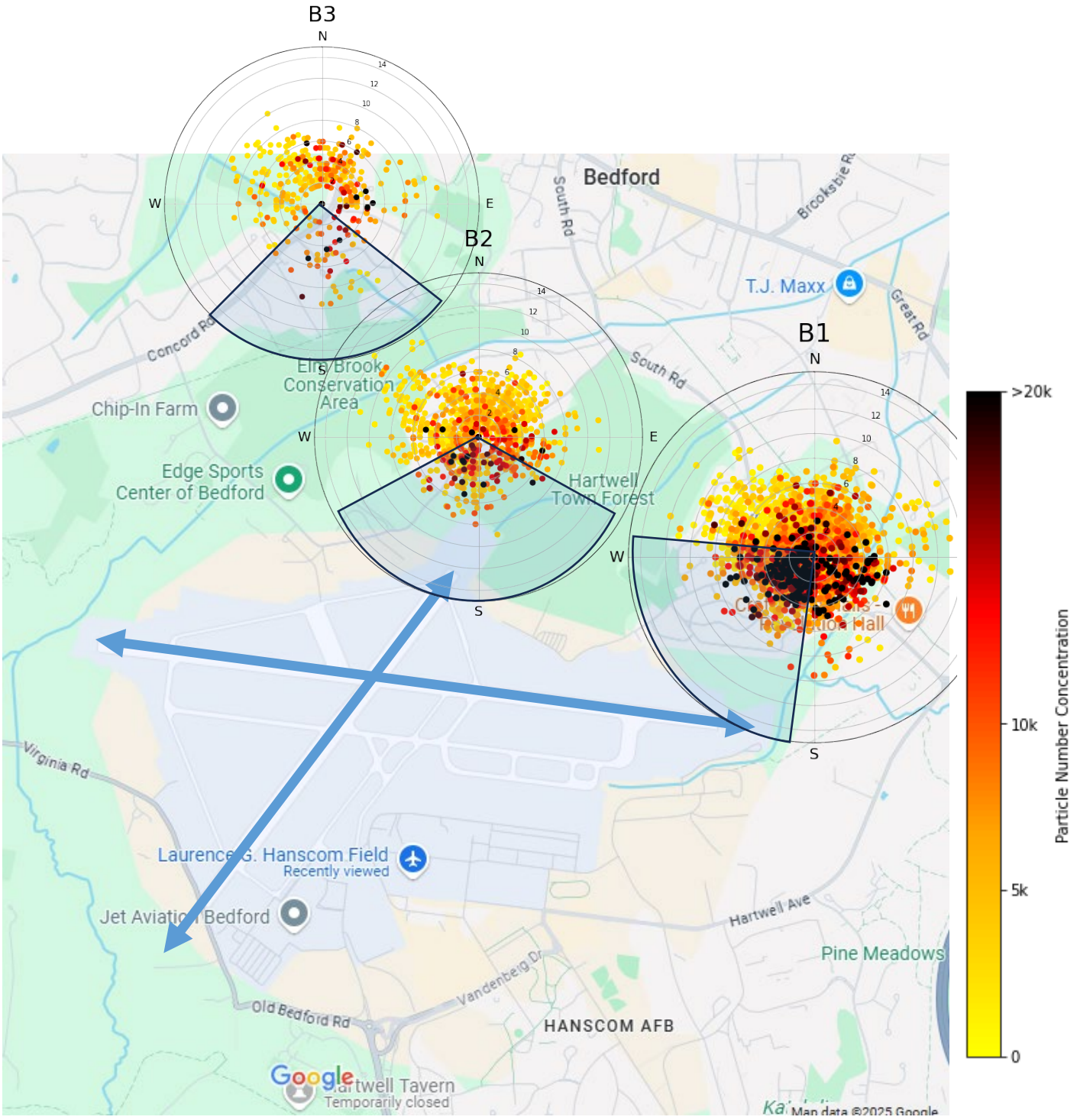

Figure A.2 Hourly average PNC polar plot for each site in Bedford. PNC is expressed in units of particles/cm^3 of air. The angular coordinate indicates the direction from which the wind is blowing, while the radial axis represents wind speed. Each point represents one hour of data; the points are colored according to the hourly average concentration. The wedge inside each plot denotes the airport impact sector.

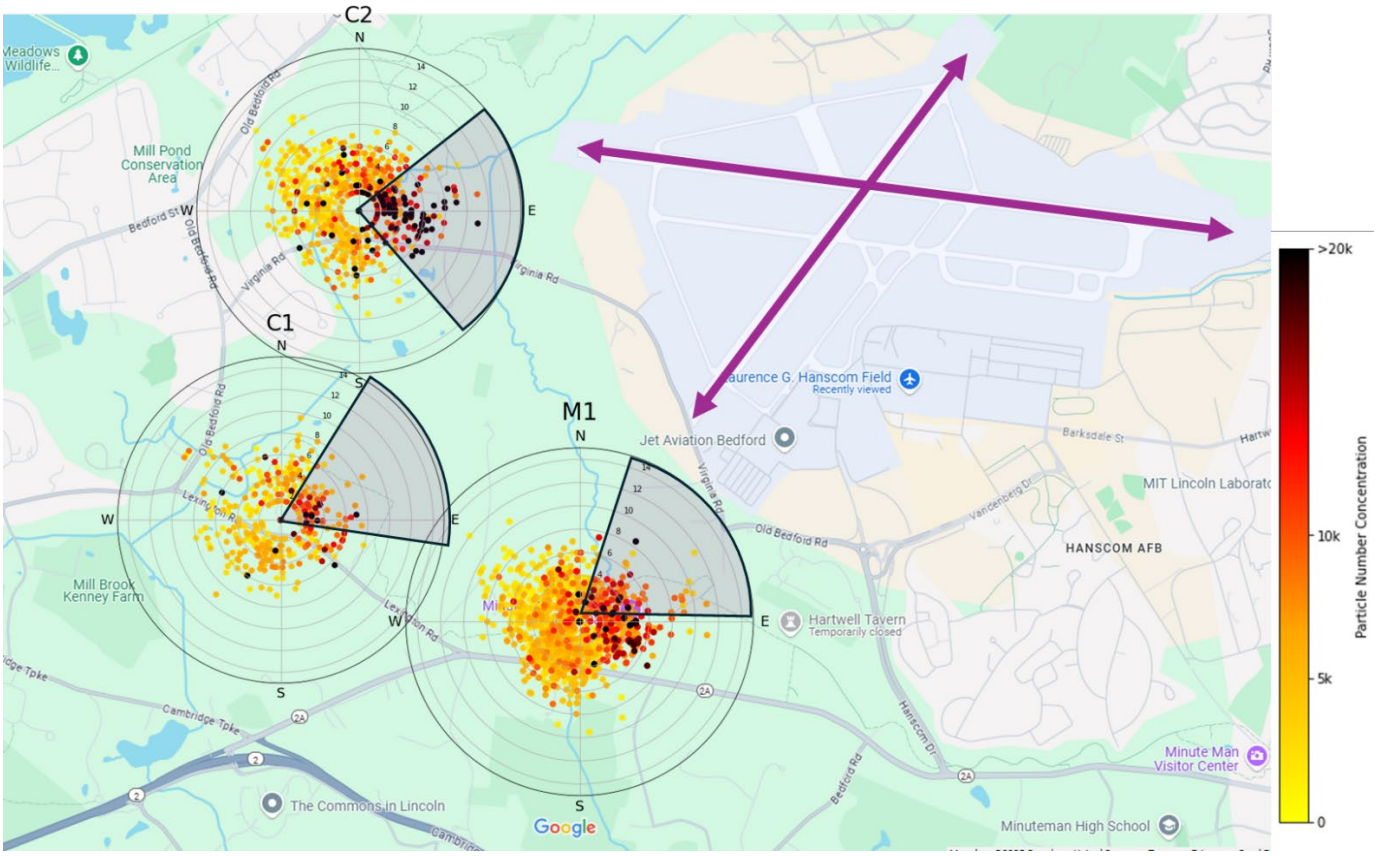

Figure A.3 Hourly average PNC polar plot for each site in Concord and Lincoln. PNC is expressed in units of particles/cm^3 of air. The angular coordinate indicates the direction from which the wind is blowing, while the radial axis represents wind speed. Each point represents one hour of data; the points are colored according to the hourly average concentration. The wedge inside each plot denotes the airport impact sector.

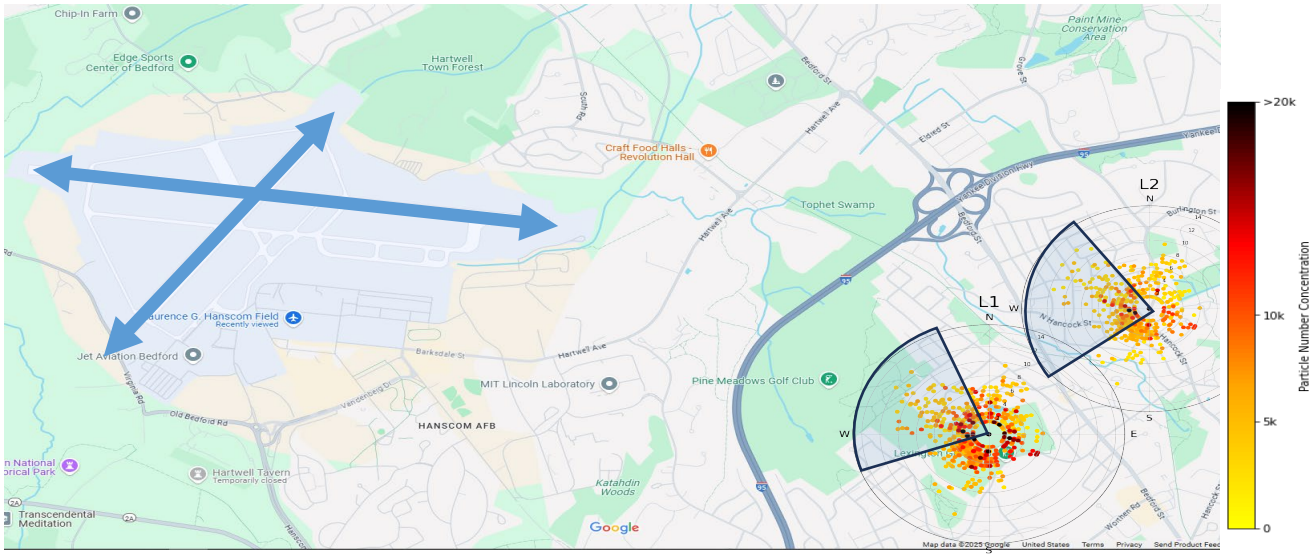

Figure A.4 Hourly average PNC polar plot for each site in Lexington. PNC is expressed in units of particles/cm^3 of air. The angular coordinate indicates the direction from which the wind is blowing, while the radial axis represents wind speed. Each point represents one hour of data; the points are colored according to the hourly average concentration. The wedge inside each plot denotes the airport impact sector.

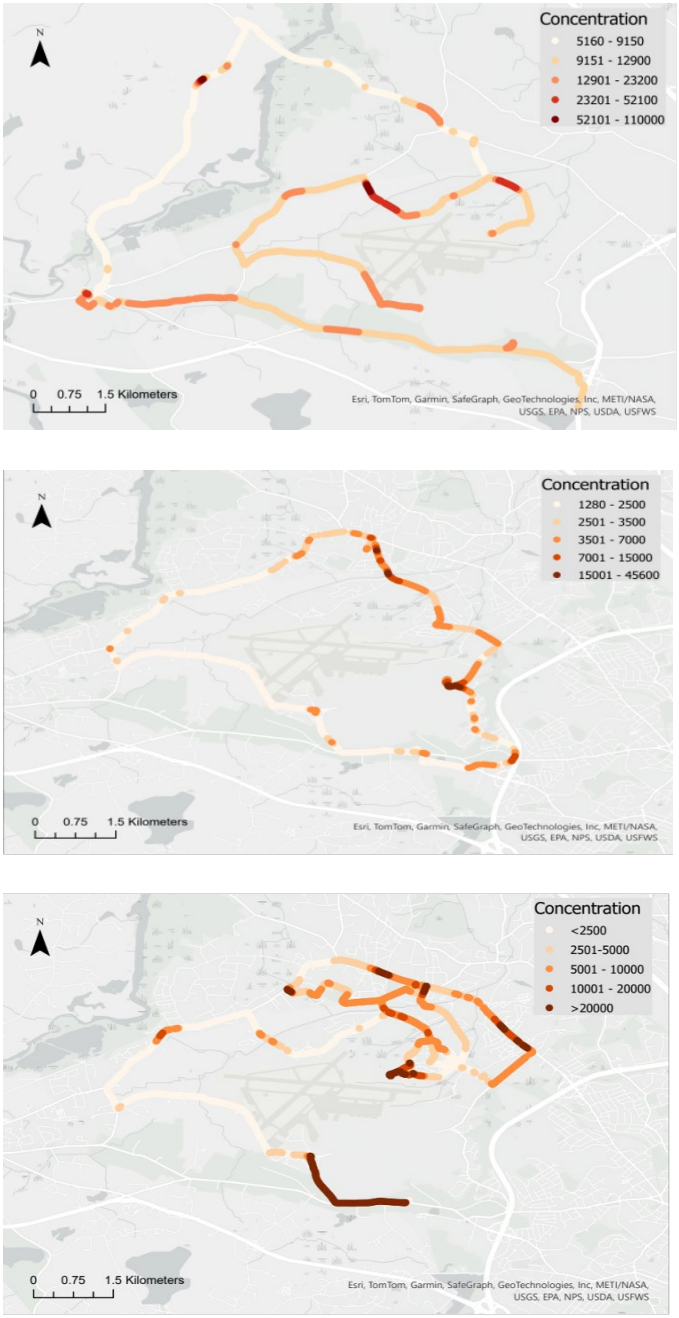

Figure A.5 Spatial distribution of ultrafine particles (particles/cm^3) based on 1-second PNC measurements made on two days of mobile monitoring in July 2024. Data in the top panel was collected on July 24th from 11:37 AM to 12:45 PM, in the middle panel on July 25th from 9:30 to 10:00 AM, and in the bottom panel from 10:10 to 11:30 AM on July 25th